

Dear Dr. Zhang:

Thanks very much for your comments and suggestions for improvement of manuscript quality. Please find below our point-by-point replies to your comments. We have addressed all the comments raised by you, and incorporated your comments / suggestions in the revised manuscript.

We are looking forward to the final acceptance of our manuscript.

Sincerely yours,

*Xuejun Liu and Wen Xu*

On behalf of all co-authors

---

**Editor Initial Decision: Reconsider after minor revisions (Editor review) (25 Oct 2015) by Leiming Zhang**

Comments to the Author:

Dear Authors,

Please consider the following comments which may help you improve the presentation quality of the paper.

1. Please rewrite the Conclusion section as detailed below (do not use the bullet point forms).

*First paragraph:* couple the first three bullets into one paragraph since all of these three bullets are on the trends (comparisons) of urban, rural and background sites. Because the trends in concentration and deposition are similar, you can combine the statements together to avoid repeating the same statement.

*Second paragraph:* Couple bullets 4 and 5 into one short paragraph.

*Third paragraph:* I think it is important to have a summary of regional pattern of atmospheric concentration and deposition. The 43 sites are located in various regions in China. A regional scale geographical pattern should be provided by comparing the same category sites (e.g., urban against urban, rural against rural, and so on).

*Fourth Paragraph:* You can point out the importance of the study (using materials in your original first paragraph), and provide some recommendations for future research directions.

**Response: We have rewritten the Conclusion section as suggested. Briefly, we do not the bullet point forms and all the paragraphs are reorganized mainly based on your suggestions in the Conclusion section. We have combined the 1<sup>st</sup> and the suggested 3<sup>rd</sup> paragraphs (a summary of regional pattern of  $N_f$  concentrations and deposition) in the Conclusion section (to avoid a too-long conclusion).**

2. Abstract: Please delete the first four lines (such information should be in the Introduction). Start the abstract with this (modified from Lines 67-71): “A Nationwide

Nitrogen Deposition Monitoring Network (NNDMN) containing 43 monitoring sites was established in China to measure gaseous  $\text{NH}_3$ ,  $\text{NO}_2$  and  $\text{HNO}_3$  and particulate  $\text{NH}_4^+$  and  $\text{NO}_3^-$  in air and precipitation from 2010 to 2014. “

**Response: Agree and revised accordingly. The revised abstract started with the following sentence: “A Nationwide Nitrogen Deposition Monitoring Network (NNDMN) containing forty-three monitoring sites was established in China to measure gaseous  $\text{NH}_3$ ,  $\text{NO}_2$  and  $\text{HNO}_3$  and particulate  $\text{NH}_4^+$  and  $\text{NO}_3^-$  in air and/or precipitation from 2010 to 2014.”**

3. Try to split the very long paragraphs (In Sections 3 and 4) into short ones for easy reading.

**Response: We have split two long paragraphs: the first paragraphs of Sections 3.1 and 4.4 into short ones for easy reading.**

1 **Quantifying atmospheric nitrogen deposition through a nationwide monitoring**  
2 **network across China**

3 W. Xu<sup>1</sup>, X. S. Luo<sup>1,2</sup>, Y. P. Pan<sup>3</sup>, L. Zhang<sup>4</sup>, A. H. Tang<sup>1</sup>, J. L. Shen<sup>5</sup>, Y. Zhang<sup>6</sup>, K. H. Li<sup>7</sup>, Q. H.  
4 Wu<sup>1</sup>, D. W. Yang<sup>1</sup>, Y. Y. Zhang<sup>1</sup>, J. Xue<sup>1</sup>, W. Q. Li<sup>8</sup>, Q. Q. Li<sup>1,9</sup>, L. Tang<sup>9</sup>, S. H. Lu<sup>10</sup>, T. Liang<sup>11</sup>, Y.  
5 A. Tong<sup>11</sup>, P. Liu<sup>12</sup>, Q. Zhang<sup>12</sup>, Z. Q. Xiong<sup>13</sup>, X. J. Shi<sup>14</sup>, L. H. Wu<sup>15</sup>, W. Q. Shi<sup>16</sup>, K. Tian<sup>17</sup>, X. H.  
6 Zhong<sup>17</sup>, K. Shi<sup>18</sup>, Q. Y. Tang<sup>19</sup>, L. J. Zhang<sup>20</sup>, J. L. Huang<sup>21</sup>, C. E. He<sup>22</sup>, F. H. Kuang<sup>23</sup>, B. Zhu<sup>23</sup>,  
7 H. Liu<sup>24</sup>, X. Jin<sup>25</sup>, Y. J. Xin<sup>25</sup>, X. K. Shi<sup>26</sup>, E. Z. Du<sup>27</sup>, A. J. Dore<sup>28</sup>, S. Tang<sup>28</sup>, J. L. Jr. Collett<sup>29</sup>, K.  
8 Goulding<sup>30</sup>, Y. X. Sun<sup>31</sup>, J. Ren<sup>32</sup>, F. S. Zhang<sup>1</sup>, X. J. Liu<sup>1,\*</sup>

9 <sup>1</sup>College of Resources and Environmental Sciences, China Agricultural University, Beijing  
10 100193, China

11 <sup>2</sup>Institute of Plant Nutrition, Resources and Environmental Sciences, Henan Academy of  
12 Agricultural Sciences, Zhengzhou 450002, China

13 <sup>3</sup>State Key Laboratory of Atmospheric Boundary Layer Physics and Atmospheric Chemistry  
14 (LAPC), Institute of Atmospheric Physics, Chinese Academy of Sciences, Beijing 100029, China

15 <sup>4</sup>Laboratory for Climate and Ocean-Atmosphere Studies, Department of Atmospheric and Oceanic  
16 Sciences, School of Physics, Peking University, Beijing 100871, China

17 <sup>5</sup>Institute of Subtropical Agriculture, Chinese Academy of Sciences, Changsha 4410125, China

18 <sup>6</sup>College of Nature Conservation, Beijing Forestry University, Beijing 100083, China

19 <sup>7</sup>Xinjiang Institute of Ecology and Geography, Chinese Academy of Sciences, Urumqi 830011,  
20 China

21 <sup>8</sup>Fujian Institute of Tobacco Agricultural Sciences, Fuzhou 350003, China

22 <sup>9</sup>College of Resources and Environmental Sciences, Yunnan Agricultural University, Kunming  
23 650224, China

24 <sup>10</sup>Soil and Fertilizer Institute, Sichuan Academy of Agricultural Sciences, Chengdu 610066, China

25 <sup>11</sup>Nature Resource and Environment College, Northwest A&F University, Yangling  
26 712100, China

27 <sup>12</sup>Institute of Agricultural Environment and Resource, Shanxi Academy of Agricultural Sciences,  
28 Taiyuan 030031, China

29 <sup>13</sup>College of Resources and Environmental Sciences, Nanjing Agricultural University, Nanjing  
30 210009, China

31 <sup>14</sup>College of Resources and Environment, Southwest University, Chongqing 400716, China

32 <sup>15</sup>College of Environmental and Resource Sciences, Zhejiang University, Hangzhou 310029,  
33 China

34 <sup>16</sup>South Subtropical Crops Research Institute, Chinese Academy of Tropical Agricultural Science,  
35 Zhanjiang 524091, China

36 <sup>17</sup>Rice Research Institute, Guangdong Academy of Agricultural Sciences, Guangzhou 510640,  
37 China

38 <sup>18</sup>College of Environmental and Chemical Engineering, Dalian Jiaotong University, Dalian

39 116028, China  
40 <sup>19</sup>College of Agriculture, Hunan Agricultural University, Changsha 410128, China  
41 <sup>20</sup>College of Resources and Environment, Agricultural University of Hebei, Baoding 071001,  
42 China  
43 <sup>21</sup>College of Plant Science and Technology, Huazhong Agricultural University, Wuhan, China  
44 <sup>22</sup>Institute of Geographic Sciences and Natural Resources, Chinese Academy of Sciences, Beijing  
45 100101, China  
46 <sup>23</sup>Institute of Mountain, Hazards and Environment, Chinese Academy of Sciences, Chengdu  
47 610041, China  
48 <sup>24</sup>Research Institute of Soil & Fertilizer and Agricultural Water Conservation, Xinjiang Academy  
49 of Agricultural Sciences, Urumqi 830091, China  
50 <sup>25</sup>The Bureau of Qinghai Meteorology, Xining 810001, China  
51 <sup>26</sup>Agriculture, Forestry and Water Department of Changdao County, Changdao 265800, China  
52 <sup>27</sup>State Key Laboratory of Earth Surface Processes and Resource Ecology, and College of  
53 Resources Science & Technology, Beijing Normal University, Beijing 100875, China  
54 <sup>28</sup>Centre for Ecology & Hydrology Edinburgh, Bush Estate, Penicuik, Midlothian EH26 0QB, UK  
55 <sup>29</sup>Department of Atmospheric Science, Colorado State University, Fort Collins, CO 80523, USA  
56 <sup>30</sup>The Sustainable Soils and Grassland Systems Department, Rothamsted Research, Harpenden  
57 AL5 2JQ, UK  
58 <sup>31</sup>Institute of Soil and Fertilizer, Anhui Academy of Agricultural Sciences, Hefei 230031, China  
59 <sup>32</sup>Institute of Soil and Fertilizer, Jilin Academy of Agricultural Sciences, Changchun 130124,  
60 China  
61 Corresponding author: liu310@cau.edu.cn (X. J. Liu).

62  
63 **Abstract:** [A Nationwide Nitrogen Deposition Monitoring Network \(NNDMN\)](#)  
64 [containing forty-three monitoring sites was established in China to measure gaseous](#)  
65 [NH<sub>3</sub>, NO<sub>2</sub> and HNO<sub>3</sub> and particulate NH<sub>4</sub><sup>+</sup> and NO<sub>3</sub><sup>-</sup> in air and/or precipitation from](#)  
66 [2010 to 2014](#). Wet/bulk deposition fluxes of N<sub>r</sub> species were collected by  
67 precipitation gauge method and measured by continuous flow analyzer; dry deposition  
68 fluxes were estimated using airborne concentration measurements and inferential  
69 models. Our observations reveal large spatial variations of atmospheric N<sub>r</sub>  
70 concentrations and dry and wet/bulk N<sub>r</sub> deposition. On a national basis, the annual  
71 average concentrations (1.3-47.0 μg N m<sup>-3</sup>) and dry plus wet/bulk deposition fluxes  
72 (2.9-83.3 kg N ha<sup>-1</sup> yr<sup>-1</sup>) of inorganic N<sub>r</sub> species ranked by land use as urban > rural >  
73 background sites [and by regions as north China > southeast China > southwest China >](#)  
74 [northeast China > northwest China > Tibetan Plateau](#), reflecting the impact of

删除的内容:

带格式的: 字体颜色: 自动设置

删除的内容:43

带格式的: 字体颜色: 自动设置

带格式的: 字体颜色: 自动设置

带格式的: 字体颜色: 自动设置

带格式的: 字体颜色: 自动设置

带格式的: 字体颜色: 自动设置

带格式的: 字体颜色: 自动设置

带格式的: 字体颜色: 自动设置

带格式的: 字体颜色: 自动设置

带格式的: 字体颜色: 自动设置

带格式的: 字体颜色: 自动设置

带格式的: 字体颜色: 自动设置

带格式的: 字体颜色: 自动设置

删除的内容: Global reactive nitrogen (N<sub>r</sub>) deposition to terrestrial ecosystems has increased dramatically since the industrial revolution. This is especially true in recent decades in China due to continuous economic growth. However, there are no comprehensive reports of both measured dry and wet/bulk N<sub>r</sub> deposition across China.

删除的内容: We therefore conducted a multiple-year study during the period mainly from 2010 to 2014 to monitor atmospheric concentrations of five major N<sub>r</sub> species of gaseous NH<sub>3</sub>, NO<sub>2</sub> and HNO<sub>3</sub>, and inorganic nitrogen (NH<sub>4</sub><sup>+</sup> and NO<sub>3</sub><sup>-</sup>) in both particles and precipitation, based on a Nationwide Nitrogen Deposition Monitoring Network (NNDMN, covering 43 sites) in China

98 anthropogenic  $N_r$  emission. Average dry and wet/bulk N deposition fluxes were 20.6  
99  $\pm 11.2$  (mean  $\pm$  standard deviation) and  $19.3 \pm 9.2$  kg N ha<sup>-1</sup> yr<sup>-1</sup> across China, with  
100 reduced N deposition dominating both dry and wet/bulk deposition. Our results  
101 suggest atmospheric dry N deposition is equally important to wet/bulk N deposition at  
102 the national scale. Therefore both deposition forms should be included when  
103 considering the impacts of N deposition on environment and ecosystem health.

104 **Keywords:** air pollution; reactive nitrogen; dry deposition; wet deposition; ecosystem;  
105 China

## 106 **1. Introduction**

107 Humans continue to accelerate the global nitrogen (N) cycle at a record pace as rates  
108 of anthropogenic reactive nitrogen ( $N_r$ ) fixation have increased 20-fold over the last  
109 century (Galloway et al., 2008). New  $N_r$  from anthropogenic fixation is formed  
110 primarily through cultivation of N-fixing legumes, the Haber-Bosch process and  
111 combustion of fossil-fuel (Galloway et al., 2013). As more  $N_r$  have been created,  
112 emissions of  $N_r$  ( $NO_x=NO+NO_2$ , and  $NH_3$ ) to the atmosphere have increased from  
113 approximately 34 Tg N yr<sup>-1</sup> in 1860 to 109 Tg N yr<sup>-1</sup> in 2010 (Fowler et al., 2013;  
114 Galloway et al., 2004); most of this emitted  $N_r$  is deposited back to land and water  
115 bodies. As an essential nutrient, N supplied by atmospheric deposition is useful for all  
116 life forms in the biosphere and may stimulate primary production in an ecosystem if it  
117 does not exceed the ecosystem-dependent critical load (Liu et al., 2010, 2011).  
118 However, long-term high levels of atmospheric  $N_r$  and its deposition can reduce  
119 biological diversity (Clark et al., 2008), degrade human health (Richter et al., 2005),  
120 alter soil and water chemistry (Vitousek et al., 1997) and influence the greenhouse gas  
121 balance (Matson et al., 2002).

122 Nitrogen deposition occurs via dry and wet processes. Neglecting dry deposition can  
123 lead to substantial underestimation of total flux as dry deposition can contribute up to  
124 2/3 of total N deposition (Flechard et al., 2011; Vet et al., 2014). For quantification of  
125 atmospheric deposition at the national scale, long-term monitoring networks such as  
126 CAPMoN (Canada), IDAF (Africa), CASTNET/NADP (the United States), EMEP  
127 (Europe) and EANET (East Asia) have been established; such networks are essential  
128 for quantification of both wet and dry deposition and revealing long-term trends and  
129 spatial patterns under major environmental and climate change (Skeffington and Hill,  
130 2012). Wet deposition, by means of rain or snow, is relatively easily measured in  
131 existing networks. In contrast, dry deposition of gases and particulate matter is much

132 more difficult to measure, and strongly influenced by factors such as surface  
133 roughness, surface wetness, and climate and environmental factors (Erisman et al.,  
134 2005). Direct methods (e.g., eddy correlation, chambers) and indirect methods (e.g.,  
135 inferential, gradient analysis) can determine dry deposition fluxes (Seinfeld and  
136 Pandis, 2006). The inferential method is widely used in many monitoring networks  
137 (e.g. CASTNET and EANET), where dry deposition rates are derived from measured  
138 ambient concentrations of  $N_r$  species and computed deposition velocities (Endo et al.,  
139 2011; Holland et al., 2005; Pan et al., 2012). Additionally, atmospheric modeling has  
140 been used as an operational tool to upscale results from sites to regions where no  
141 measurements are available (Flechard et al., 2011; Zhao et al., 2015).

142 According to long-term trends observed by the above monitoring networks, N  
143 deposition has decreased over the last two decades in Europe (EEA, 2011).  
144 Measurements of wet deposition in the US show a strong decrease in  $NO_3$ -N  
145 deposition over most of the country (Du et al., 2014), but  $NH_4$ -N deposition increased  
146 in agricultural regions. China, as one of the most rapidly developing countries in East  
147 Asia, has witnessed serious atmospheric  $N_r$  pollution since the late 1970s (Hu et al.,  
148 2010; Liu et al., 2011). Accurate quantification of N deposition is key to assessing its  
149 ecological impacts on terrestrial ecosystems (Liu et al., 2011). Previous modeling  
150 studies (e.g., Dentener et al., 2006; Galloway et al., 2008; Vet et al., 2014) suggested  
151 that central-east China was a global hotspot for N deposition. More recently, based on  
152 meta-analyses of historic literature, both Liu et al. (2013) and Jia et al. (2014)  
153 reported a significant increase in N wet/bulk deposition in China since the 1980s or  
154 1990s. However, most measurements in China only reported wet/bulk deposition (e.g.,  
155 Chen et al., 2007; Huang et al., 2013; Zhu et al., 2015) and/or dry deposition (Luo et  
156 al., 2013; Shen et al., 2009; Pan et al., 2012) at a local or regional scale. Although  
157 national N deposition has been investigated by Lü and Tian (2007, 2014), the  
158 deposition fluxes were largely underestimated due to the inclusion only of gaseous  
159  $NO_2$  in dry deposition and not  $NH_3$ ,  $HNO_3$  and particulate ammonium and nitrate etc.  
160 Therefore, the magnitude and spatial patterns of *in-situ* measured N wet /bulk and dry  
161 deposition across China are still not clear.

162 Against such a background, we have established a Nationwide Nitrogen Deposition  
163 Monitoring Network (NNDMN) in China since 2010, measuring both wet/bulk and  
164 dry deposition. The NNDMN consists of forty-three *in-situ* monitoring sites, covering  
165 urban, rural (cropland) and background (coastal, forest and grassland) areas across

删除的内容: Zhang et al., 2012a;

删除的内容:

删除的内容:

169 China. The focus of the network is to conduct high-quality measurements of  
170 atmospheric  $N_r$  in gases, particles and precipitation. These data provide a unique and  
171 valuable quantitative description of  $N_r$  deposition in China, but have never been  
172 published as a whole. The objectives of this study were therefore to: (1) obtain the  
173 first quantitative information on atmospheric  $N_r$  concentrations and pollution status  
174 across China; and (2) analyze overall fluxes and spatial variations of N wet/bulk and  
175 dry deposition in relation to anthropogenic  $N_r$  emissions from different regions,

删除的内容: in and among

删除的内容: as well as on a national basis

## 176 2. Materials and Methods

### 177 2.1 Sampling sites

178 The distribution of the forty-three monitoring sites in the NNDMN is shown in **Fig. 1**.  
179 Although sampling periods varied between sites, most of our monitoring started from  
180 2010 to 2014 (see Supporting Materials for details). The NNDMN comprise 10 urban  
181 sites, 22 rural sites and 11 background sites (**Table S1** of the online Supplement). To  
182 better analyze atmospheric N deposition results among the sites, we divided the  
183 forty-three sites into six regions: north China (NC, 13 sites), northeast China (NE, 5  
184 sites); northwest China (NW, 6 sites), southeast China (SE, 11 sites), southwest China  
185 (SW, 6 sites), and Tibetan Plateau (TP, 2 sites), representing China's various  
186 social-economical and geo-climatic regions (for details, see **Sect. A1** of the online  
187 Supplement). The sites in the six regions are described using region codes (i.e., NC,  
188 NE, NW, SE, SW, TP) plus site numbers such as NC1, NC2, NC3, ..., NE1, NE2, etc.  
189 The longitudes and latitudes of all 43-sites ranged from 83.71 to 129.25 °E, and from  
190 21.26 to 50.78 °N, respectively. Annual mean rainfall ranged from 170 to 1748 mm  
191 and the annual mean air temperature ranged from -6.2 to 23.2 °C. Site names, land use  
192 types and population densities are summarized in **Table S1** of the Supplement. More  
193 detailed information on the monitoring sites, such as specific locations, surrounding  
194 environment and possible emission sources are provided in **Sect. A2** of the  
195 Supplement.

### 196 2.2 Collection of gaseous and particulate $N_r$ samples

197 In this study ambient  $N_r$  concentrations of gaseous  $NH_3$ ,  $NO_2$  and  $HNO_3$ , and  
198 particulate  $NH_4^+$  ( $pNH_4^+$ ) and  $NO_3^-$  ( $pNO_3^-$ ) were measured monthly at the 43 sites  
199 using continuous active and passive samplers. DELTA active sampling systems  
200 (DENuder for Long-Term Atmospheric sampling, described in detail in [Flechard et al.](#)  
201 [\(2011\)](#) and [Sutton et al. \(2001\)](#)), were used to collect  $NH_3$ ,  $HNO_3$ ,  $pNH_4^+$  and  $pNO_3^-$ ;  
202  $NO_2$  samples were collected using Gradko diffusion tubes ([Gradko International](#)

206 Limited, UK) at all sampling sites. The air intakes of the DELTA system and the NO<sub>2</sub>  
207 tubes were set at a height of 2 m above the ground (at least 0.5 m higher than the  
208 canopy height) at most sites. At a few sites, the DELTA systems could not be used due  
209 to power constraints. Therefore, NH<sub>3</sub> samples were collected using ALPHA passive  
210 samplers (Adapted Low-cost High Absorption, designed by the Center for Ecology  
211 and Hydrology, Edinburgh, UK), while the pNH<sub>4</sub><sup>+</sup> and pNO<sub>3</sub><sup>-</sup> in PM<sub>10</sub> were collected  
212 using particulate samplers (TSH-16 or TH-150III, Wuhan Tianhong Corp., Wuhan,  
213 China). However, HNO<sub>3</sub> measurements were not performed due to lack of  
214 corresponding passive samplers. Briefly, all the measurements of N<sub>r</sub> concentration  
215 were based on monthly sampling (one sample per month for each N<sub>r</sub> species) except  
216 at the very few sites without DELTA systems, where pNH<sub>4</sub><sup>+</sup> and pNO<sub>3</sub><sup>-</sup> samples were  
217 calculated from daily sampling transformed to monthly averaged data. Detailed  
218 information on measuring methods, sample replication and collection are given in  
219 **Sect. A3** of the Supplement with sampling periods listed in **Table S2** of the  
220 Supplement. Comparisons between the ALPHA samplers and the DELTA systems at  
221 six network sites for gaseous NH<sub>3</sub> measurements indicated that the two methods  
222 provided comparable NH<sub>3</sub> concentrations (values between the two methods were not  
223 significantly different) (cf. **Sect. A4** in the Supplement and **Fig. S1** therein).

### 224 *2.3 Collection of precipitation*

225 At all monitoring sites precipitation (here we define it as wet/bulk deposition which  
226 contains wet and part dry deposition) samples were collected using precipitation  
227 gauges (SDM6, Tianjin Weather Equipment Inc., China) located beside the DELTA  
228 systems (c. 2 m). The collector, consisting of a stainless steel funnel and glass bottle  
229 (vol. 2000-2500 ml), collects precipitation (rainwater, snow) without a power supply.  
230 Precipitation amount was measured using a graduated cylinder (scale range: 0-10 mm;  
231 division: 0.1 mm) coupled with the gauge. After each daily (8:00 am-8:00 am next  
232 day) event, the collected samples were thoroughly mixed and then immediately stored  
233 in clean polyethylene bottles (50 mL). All collected samples (including melted snow)  
234 samples were frozen at -18 °C at each site until delivery to the laboratory at China  
235 Agricultural University (CAU) for analysis of inorganic N (NH<sub>4</sub><sup>+</sup> and NO<sub>3</sub><sup>-</sup>). The  
236 gauges were cleaned with high-purity water after each collection and once every week  
237 in order to avoid cross contamination.

### 238 *2.4 Analytical procedures*

239 In CAU's analytical laboratory, the exposed sampling trains of the DELTA systems



240 and passive samples were stored at 4 °C and analyzed at one-month intervals. The  
241 HNO<sub>3</sub> denuders and alkaline-coated filters were extracted with 10 mL 0.05 % H<sub>2</sub>O<sub>2</sub>  
242 in aqueous solution. The NH<sub>3</sub> denuders and acid-coated filters, and ALPHA samplers  
243 were extracted with 10 mL high-purity water. The loaded PM<sub>10</sub> filters were extracted  
244 with 50 mL high-purity water by ultrasonication for 30-60 min and then filtered  
245 through a syringe filter (0.45 μm, Tengda Inc., Tianjin, China). Ammonium (NH<sub>4</sub><sup>+</sup>)  
246 and nitrate (NO<sub>3</sub><sup>-</sup>) in the extracted and filtered solutions were measured with an AA3  
247 continuous-flow analyzer (Bran+Luebbe GmbH, Norderstedt, Germany). The  
248 detection limits were 0.01 mg N L<sup>-1</sup> for NH<sub>4</sub><sup>+</sup> and NO<sub>3</sub><sup>-</sup>. It should be noted that  
249 NO<sub>3</sub><sup>-</sup> was converted to NO<sub>2</sub><sup>-</sup> during the chemical analysis. So, NO<sub>2</sub><sup>-</sup> here was included  
250 in the analysis, and NO<sub>3</sub><sup>-</sup> equals to the sum of NO<sub>2</sub><sup>-</sup> and NO<sub>3</sub><sup>-</sup>. The disks from the  
251 Gradko samplers were extracted with a solution containing sulphanilamide, H<sub>3</sub>PO<sub>4</sub>  
252 and N-1-Naphthylethylene-diamine, and the NO<sub>2</sub><sup>-</sup> content in the extract determined  
253 using a colorimetric method by absorption at a wavelength of 542 nm. The detection  
254 limit for NO<sub>2</sub><sup>-</sup> was 0.01 mg N L<sup>-1</sup>. Three laboratory and three field blank samples  
255 were extracted and analyzed using the same methods as the exposed samples. After  
256 correcting for the corresponding blanks, the results were used for the calculation of  
257 ambient concentrations of gaseous and particulate N<sub>r</sub>. Each collected precipitation  
258 sample was filtered with a 0.45 μm syringe filter, and 15 mL filtrates frozen and  
259 stored in polypropylene bottles until chemical analysis within one month. The NH<sub>4</sub><sup>+</sup>  
260 and NO<sub>3</sub><sup>-</sup> concentrations of the filtrates were determined using an AA3  
261 continuous-flow analyzer as described above.

### 262 2.5 Deposition flux estimation

263 The inferential technique, which combines the measured concentration and a modeled  
264 dry deposition velocity (V<sub>d</sub>), was used to estimate the dry deposition fluxes of N<sub>r</sub>  
265 species (Schwede et al., 2011; Pan et al., 2012). The concentrations of gases (HNO<sub>3</sub>,  
266 NO<sub>2</sub> and NH<sub>3</sub>) and aerosols (NH<sub>4</sub><sup>+</sup> and NO<sub>3</sub><sup>-</sup>) were measured as described in Section  
267 2.2. The monthly average V<sub>d</sub> over China was calculated by the GEOS-Chem chemical  
268 transport model (CTM) (Bey et al., 2001; <http://geos-chem.org>). The GEOS-Chem  
269 CTM is driven by GEOS-5 (Goddard Earth Observing System) assimilated  
270 meteorological data from the NASA Global Modeling and Assimilation Office  
271 (GMAO) with a horizontal resolution of 1/2° latitude × 2/3° longitude and 6-h  
272 temporal resolution (3-h for surface variables and mixing depths). We used a  
273 nested-grid version of GEOS-Chem for Asia that has the native 1/2°×2/3° resolution

274 over East Asia (70°E-150°E, 11°S-55°N) (Chen et al., 2009). The nested model has  
275 been applied to examine atmospheric N<sub>r</sub> deposition to the northwestern Pacific (Zhao  
276 et al., 2015), and a similar nested model for North America has been used to analyze  
277 N<sub>r</sub> deposition over the United States (Zhang et al., 2012a; Ellis et al., 2013). The  
278 model calculation of dry deposition of N<sub>r</sub> species follows a standard big-leaf  
279 resistance-in-series model as described by Wesely (1989) for gases and Zhang et al.  
280 (2001) for aerosol. For a detailed description of the V<sub>d</sub> calculation as well as the  
281 estimation of N dry deposition, the reader is referred to the Supplement (Sect. A5),  
282 with monthly and annual dry deposition velocities of N<sub>r</sub> for different land use types  
283 presented in Tables S3 and S4 therein. The model uses the land map of the Global  
284 Land Cover Characteristics Data Base Version 2.0  
285 ([http://edc2.usgs.gov/glcc/globdoc2\\_0.php](http://edc2.usgs.gov/glcc/globdoc2_0.php)), which defines the land types (e.g., urban,  
286 forest, etc.) at the native 1 km × 1 km resolution and is then binned to the model  
287 resolution as a fraction of the grid cell covered by each land type. The model 1/2°  
288 resolution may coarsely represent the local land characteristics at the monitoring sites.  
289 Future work using a single-point dry deposition model as for CASTNET (Clarke et al.,  
290 1997) would further improve the dry deposition flux estimates, but that requires  
291 concurrent *in-situ* measurements of meteorological variables which are not available  
292 at present.

293 Wet/bulk N deposition flux was calculated as the product of the precipitation amount  
294 and the concentration of N<sub>r</sub> species in precipitation, using the following equations (1)  
295 and (2):

$$296 C_w = \sum_{i=1}^n (C_i P_i) / \sum_{i=1}^n P_i \quad (1)$$

297 where  $C_w$  is the volume-weighted mean (VWM) concentration (mg N L<sup>-1</sup>) calculated  
298 from the  $n$  precipitation samples within a month or a year, and the individual sample  
299 concentration  $C_i$  is weighted by the rainfall amount  $P_i$  for each sample.

$$300 D_w = P_t C_w / 100 \quad (2)$$

301 where  $D_w$  is the wet/bulk deposition flux (kg N ha<sup>-1</sup>),  $P_t$  is the total amount of all  
302 precipitation events (mm), and 100 is a unit conversion factor.

### 303 2.6 Statistics

304 A one-way analysis of variance (ANOVA) and nonparametric t-tests were conducted  
305 to examine the differences in the investigated variables between sites (urban, rural and  
306 background) and between the six regions. Linear regression analysis was used to

删除的内容: nitrogen

删除的内容: nitrogen

删除的内容: 2012b

带格式的: 字体颜色: 蓝色

带格式的: 字体颜色: 蓝色

310 analyze the relationships among annual wet N deposition flux, annual precipitation  
311 amount and annual VWM concentration of inorganic N in precipitation. All analyses  
312 were performed using SPSS 11.5 (SPSS Inc., Chicago, IL, USA). Statistically  
313 significant differences were set at  $P$  values  $< 0.05$ .

### 314 **3. Results**

#### 315 *3.1 Concentrations of $N_r$ species in air*

316 Monthly mean concentrations of  $\text{NH}_3$ ,  $\text{NO}_2$ ,  $\text{HNO}_3$ ,  $\text{pNH}_4^+$  and  $\text{pNO}_3^-$  were  
317 0.08-34.8, 0.13-33.4, 0.02-4.90, 0.02-55.0 and 0.02-32.1  $\mu\text{g N m}^{-3}$ , respectively (**Fig.**  
318 **S2a-e**, Supplement). The annual mean concentrations of gaseous and particulate  $N_r$   
319 were calculated for each site from the monthly  $N_r$  concentrations (**Fig. 2a**), and  
320 further were averaged for land use types in the six regions (**Fig. 3a-e**) and the whole  
321 nation (**Fig. 4a**) according to geographical location and the classification of each site.  
322 Annual mean  $\text{NH}_3$  concentrations ranged from 0.3 to 13.1  $\mu\text{g N m}^{-3}$ , with an overall  
323 average value of 6.1  $\mu\text{g N m}^{-3}$ . In NC, SE and SW, the  $\text{NH}_3$  concentrations at the  
324 urban sites (average for the three regions,  $9.5 \pm 2.1 \mu\text{g N m}^{-3}$ ) were about 1/3 higher  
325 than at the rural sites ( $6.2 \pm 2.3 \mu\text{g N m}^{-3}$ ) and were almost twice of those at the  
326 background sites ( $4.8 \pm 1.4 \mu\text{g N m}^{-3}$ ), whereas in NE and NW  $\text{NH}_3$  concentrations  
327 were lower at the urban sites (average of the two regions,  $5.5 \pm 3.2 \mu\text{g N m}^{-3}$ ) than at  
328 the rural sites ( $8.8 \pm 0.3 \mu\text{g N m}^{-3}$ ) but 4.6-times greater than at the background sites  
329 ( $1.2 \pm 0.5 \mu\text{g N m}^{-3}$ ). Comparing land use types by region, annual  $\text{NH}_3$  concentrations  
330 at the rural sites in northern regions (NC, NE and NW) were approximately equal,  
331 which on average were 1.8-times greater than the average of southern rural sites. In  
332 contrast, annual  $\text{NH}_3$  concentrations at urban and background sites ranked in the order:  
333  $\text{SW} > \text{NC} > \text{NW} > \text{SE} > \text{TP} > \text{NE}$ , and  $\text{SW} > \text{NC} > \text{SE} > \text{NW} > \text{TP} > \text{NE}$ , respectively  
334 (**Fig. 3a**).

335 Annual mean  $\text{NO}_2$  concentrations showed similar spatial variations (0.4 to 16.2  $\mu\text{g N}$   
336  $\text{m}^{-3}$ ) to those of  $\text{NH}_3$ , and overall averaged 6.8  $\mu\text{g N m}^{-3}$ . In the six regions, the  $\text{NO}_2$   
337 concentrations at urban sites were 1.4-4.5 times higher than those at rural sites, and  
338 were even 2.0-16.6 times higher than the background sites (except for SW). By  
339 comparison among regions, annual mean  $\text{NO}_2$  concentrations at rural sites in NC were  
340 about 2.6-times higher than in NE and NW, and overall averaged  $\text{NO}_2$  concentrations  
341 in northern rural China (NC, NE and NW,  $5.7 \pm 3.5 \mu\text{g N m}^{-3}$ ) were comparable to  
342 those at southern rural sites (average of SE and SW,  $5.1 \pm 0.1 \mu\text{g N m}^{-3}$ ). As for urban  
343 and background sites, the annual mean  $\text{NO}_2$  concentrations followed the order:  $\text{NC} >$

344 NW > SE > SW > NE > TP, and SW > NC > SE > NE > NW > TP, respectively (**Fig.**  
345 **3b**).

346 Annual mean HNO<sub>3</sub> concentrations were relatively low everywhere (from 0.1 to 2.9  
347 μg N m<sup>-3</sup>, average 1.3 μg N m<sup>-3</sup>). In all regions except NE and TP, the HNO<sub>3</sub>  
348 concentrations were highest at the urban sites (1.7-2.4 μg N m<sup>-3</sup>), followed by the  
349 rural sites (0.8-1.6 μg N m<sup>-3</sup>), and were lowest at the background sites (0.2-1.1 μg N  
350 m<sup>-3</sup>). The HNO<sub>3</sub> concentrations were comparable for the same land use types across  
351 northern and southern monitoring sites, on average, 1.8 vs. 1.8, 1.2 vs. 1.0, and 0.6 vs.  
352 0.8 μg N m<sup>-3</sup> at the urban, rural and background sites, respectively (**Fig. 3c**). The  
353 annual mean concentrations of pNH<sub>4</sub><sup>+</sup> and pNO<sub>3</sub><sup>-</sup> were in the ranges of 0.2-18.0 μg N  
354 m<sup>-3</sup> (average 5.7 μg N m<sup>-3</sup>) and 0.2-7.7 μg N m<sup>-3</sup> (average 2.7 μg N m<sup>-3</sup>), respectively.  
355 Annual pNH<sub>4</sub><sup>+</sup> concentrations show a decreasing trend of urban > rural > background  
356 in all regions (except NE), where relatively higher concentrations were observed at  
357 the rural sites than the urban sites, and in SE, where no clear differences were  
358 observed among three land use types (**Fig. 3d**). In contrast, annual  
359 pNO<sub>3</sub><sup>-</sup> concentrations showed a declining trend of urban > rural > background in all  
360 regions (**Fig. 3e**). Overall, annual mean concentrations of both pNH<sub>4</sub><sup>+</sup> and pNO<sub>3</sub><sup>-</sup> at  
361 all land use types were both slightly higher in northern China (NC, NE and NW) than  
362 in southern China (SE, SW and TP).

363 In total, annual mean concentrations of gaseous and particulate N<sub>r</sub> in air were 1.3-47.0  
364 μg N m<sup>-3</sup> among all sampling sites. The total annual concentrations of measured N<sub>r</sub>  
365 generally decreased in the order of urban > rural > background in all regions except  
366 NE (**Fig. 3f**).

### 367 3.2 Concentrations of N<sub>r</sub> species in precipitation

368 The monthly VWM concentrations of inorganic N<sub>r</sub> species at the forty-three sampling  
369 sites during the study period ranged from 0.01 to 27.1 mg N L<sup>-1</sup> for NH<sub>4</sub><sup>+</sup>-N and from  
370 0.02 to 27.9 mg N L<sup>-1</sup> for NO<sub>3</sub><sup>-</sup>-N (**Fig. S3**, Supplement). The annual VWM  
371 concentrations of NH<sub>4</sub><sup>+</sup>-N and NO<sub>3</sub><sup>-</sup>-N across all sites were in the ranges of 0.2-4.3  
372 and 0.1-2.5 mg N L<sup>-1</sup>, respectively, with averages of 1.6 and 1.3 mg N L<sup>-1</sup> (**Fig. 2b**).  
373 The urban-rural-background distributions of annual VWM concentrations of NH<sub>4</sub><sup>+</sup>-N  
374 and NO<sub>3</sub><sup>-</sup>-N were, respectively, fairly coincided with corresponding reduced (i.e. NH<sub>3</sub>  
375 and pNH<sub>4</sub><sup>+</sup>) and oxidized N<sub>r</sub> (i.e. HNO<sub>3</sub> and pNO<sub>3</sub><sup>-</sup>) in all regions except NH<sub>4</sub><sup>+</sup>-N in  
376 SE and NO<sub>3</sub><sup>-</sup>-N in NW (**Figs. 3g and h**). Conversely, the regional variations in annual  
377 VWM concentrations of NH<sub>4</sub><sup>+</sup>-N and NO<sub>3</sub><sup>-</sup>-N for the three land use types were not

删除的内容: ing

删除的内容: averages:

380 consistent with corresponding reduced and oxidized  $N_r$ , respectively. On a national  
381 basis, the VWM concentrations of  $NH_4^+$ -N and  $NO_3^-$ -N were both decreased in the  
382 order urban  $\geq$  rural  $>$  background (**Fig. 4b**). The annual total inorganic N (TIN)  
383 concentrations in precipitation across all sites were 0.4-6.0 mg N L<sup>-1</sup>, decreasing from  
384 urban to background sites in all regions (except NE) as well as on a national basis  
385 (**Figs. 3i and 4b**).

### 386 3.3 Dry deposition of $N_r$ species

387 The dry deposition fluxes of  $NH_3$ ,  $NO_2$ ,  $HNO_3$ ,  $pNH_4^+$  and  $pNO_3^-$  were in the ranges  
388 of 0.5-16.0, 0.2-9.8, 0.2-16.6, 0.1-11.7 and 0.1-4.5 kg N ha<sup>-1</sup> yr<sup>-1</sup>, and averaged 8.2,  
389 3.2, 5.4, 3.2 and 1.5 kg N ha<sup>-1</sup> yr<sup>-1</sup>, respectively (**Fig. 5a**). The total dry N deposition  
390 across all sites ranged from 1.1 to 52.2 kg N ha<sup>-1</sup> yr<sup>-1</sup> (average, 20.6  $\pm$  11.2 kg N ha<sup>-1</sup>  
391 yr<sup>-1</sup>). Gaseous N species were the primary contributors to total dry-deposited N,  
392 ranging from 60% to 96%, despite of the missing  $HNO_3$  data at a few sites. In general,  
393  $NH_3$  was predominant  $N_r$  species in total dry N deposition and accounted for 24-72%,  
394 compared with 1-43% from  $NO_2$  and 9-37% from  $HNO_3$ . Comparing land use types  
395 in each region, spatial pattern of individual fluxes is fairly consistent with that of their  
396 respective concentrations except that of  $NH_3$  for NC, that of  $NO_2$  for SW, those of  
397  $NO_2$  and  $pNH_4^+$  for NW and those of almost all measured  $N_r$  species for NE (**Figs.**  
398 **3a-e and 6a-e**). Furthermore, a consistent picture is also seen for the total flux (sum  
399 of fluxes of five  $N_r$  species) at each land use type (**Figs. 5f and 6f**). Among the six  
400 regions, regional variations of individual fluxes at each land use type generally  
401 differed from those of their respective concentrations. Similarly, the inconsistent  
402 behavior appeared for the total fluxes at urban and rural sites but not at background  
403 site. On a national basis, there was no significant difference ( $p>0.05$ ) in the total dry  
404 N deposition fluxes between urban (26.9 kg N ha<sup>-1</sup> yr<sup>-1</sup>) and rural (23.0 kg N ha<sup>-1</sup> yr<sup>-1</sup>)  
405 sites, both of which were significantly higher than background site (10.1 kg N ha<sup>-1</sup>  
406 yr<sup>-1</sup>). Also, a similar pattern was found for the dry deposition flux of each  $N_r$  species  
407 among different land use types (**Fig. 4c**).

### 408 3.4 Wet/bulk deposition of $N_r$ species

409 Wet/bulk N deposition fluxes at the forty-three sites ranged from 1.0 to 19.1 kg N ha<sup>-1</sup>  
410 yr<sup>-1</sup> for  $NH_4^+$ -N and from 0.5 to 20.1 kg N ha<sup>-1</sup> yr<sup>-1</sup> for  $NO_3^-$ -N (**Fig. 5b**). The annual  
411 wet/bulk deposition fluxes of  $NH_4^+$ -N were, on average, 1.3 times those of  $NO_3^-$ -N.  
412 The total wet/bulk N ( $NH_4^+$ -N +  $NO_3^-$ -N) deposition fluxes across all the sites were

删除的内容: annual

删除的内容: d

删除的内容: Annual w

删除的内容: annual

417 1.5-32.5 kg N ha<sup>-1</sup> yr<sup>-1</sup> (average 19.3 kg N ha<sup>-1</sup> yr<sup>-1</sup>), with a large spatial variation.  
418 Region variation of annual wet/bulk N deposition followed the order of NC > SE >  
419 SW > NE > NW > TP for NH<sub>4</sub><sup>+</sup>-N, and SE > NC > SW > NE > TP > NW for NO<sub>3</sub><sup>-</sup>-N,  
420 both of which differed from their orders of annual VWM concentration, reflecting  
421 differences in annual precipitation amount. Annual total wet/bulk N deposition fluxes  
422 averaged 24.6, 13.6, 7.4, 24.4, 17.6 and 7.6 kg N ha<sup>-1</sup> yr<sup>-1</sup>, respectively, in NC, NE,  
423 NW, SE, SW and TP (**Fig. 5b**). At national scale, annual wet/bulk deposition fluxes of  
424 total inorganic N and/or each N<sub>r</sub> species at urban and rural sites were comparable but  
425 significantly higher (*p*<0.05) than those at background sites (**Fig. 4d**).

### 426 3.5 Total annual dry and wet/bulk deposition of N<sub>r</sub> species

427 The total (dry plus wet/bulk) N deposition at the forty-three sites ranged from 2.9 to  
428 83.3 kg N ha<sup>-1</sup> yr<sup>-1</sup> (average 39.9 kg N ha<sup>-1</sup> yr<sup>-1</sup>) for the period, with 23-83%  
429 dry-deposited (**Fig. 5c**). Separated by land use types or regions, total annual mean N  
430 deposition fluxes were 49.7, 44.3 and 26.0 kg N ha<sup>-1</sup> at the urban, rural and  
431 background sites, or 56.2, 41.7, 37.8, 27.6, 18.8, 15.2 kg N ha<sup>-1</sup> in NC, SE, SW, NE,  
432 NW and TP, respectively, reflecting different anthropogenic impacts. In our network,  
433 the NH<sub>x</sub> (i.e. wet/bulk NH<sub>4</sub><sup>+</sup>-N deposition plus dry deposition of NH<sub>3</sub> and particulate  
434 NH<sub>4</sub><sup>+</sup>)/NO<sub>y</sub> (wet/bulk NO<sub>3</sub><sup>-</sup>-N deposition plus dry deposition of NO<sub>2</sub>, HNO<sub>3</sub> and  
435 particulate NO<sub>3</sub><sup>-</sup>) ratio at urban sites (from 0.8 to 1.8, averaging 1.2) was not  
436 significantly different (*p*>0.05) from rural (from 0.5 to 2.7, averaging 1.3) and  
437 background (from 1.0 to 2.5, averaging 1.6) sites. On a regional basis, the relative  
438 importance of dry vs. wet/bulk N deposition to the total deposition were different in  
439 the six regions, 57% vs. 43% in NC, 54% vs. 46% in NE, 61% vs. 39% in NW, 42%  
440 vs. 58% in SE, 55% vs. 45% in SW, and 50% vs. 50% in TP (**Fig. 7**).

## 441 4. Discussion

### 442 4.1 Concentration of N<sub>r</sub> species in air and precipitation

443 China is facing serious atmospheric N<sub>r</sub> pollution induced by anthropogenic N<sub>r</sub>  
444 emissions (Liu et al., 2011, 2013). The present study shows that monthly N<sub>r</sub>  
445 concentrations of species, through comparisons among regions, have a distinct spatial  
446 variability with values significantly higher (all *p*<0.05) in NC and significantly lower  
447 (all *p*<0.05) in TP. Annual mean NH<sub>3</sub> and NO<sub>2</sub> concentrations at most sampling sites  
448 are in good agreement with the emission inventory and satellite observations by Gu et  
449 al. (2012), who reported NH<sub>3</sub> hotspots in the North China Plain and South Central  
450 China such as Jiangsu and Guangdong provinces, while NO<sub>x</sub> hotspots were mainly in

删除的内容: annual

删除的内容: 43

453 more developed regions such as the Jing-Jin-Ji (Beijing-Tianjin-Hebei), the Yangtze  
454 River Delta and the Pearl River Delta. Our results confirm that NC, which consumes  
455 large quantities of fertilizers (for food production) and fossil fuel (for energy supply)  
456 (Zhang et al., 2010) experiences the most serious  $N_r$  pollution in China; TP is the least  
457 polluted region due to much less human activity. When considering different land use  
458 types, the average total annual  $N_r$  concentrations ranked urban > rural > background,  
459 with significant differences (all  $p < 0.05$ ) among them, despite site-to-site variability  
460 within regions. This reflects the dominant role of human activity on atmospheric  $N_r$ .

461 For individual  $N_r$  species, higher mean concentrations were observed at urban sites  
462 than at rural and background sites (Fig. 4a). Higher  $NH_3$  concentration in urban areas  
463 may be associated with  $NH_3$  emissions from biological sources, such as human,  
464 sewage disposal systems and refuse containers (Reche et al., 2002). In addition,  $NH_3$   
465 can be produced by over-reduction of NO in automobile catalytic converters (Behera  
466 et al., 2013), increasing ambient  $NH_3$  concentrations in urban areas with high traffic  
467 densities. Between 2006 and 2013, the number of civil vehicles increased from 2.39 to  
468 5.17 million in Beijing and from 0.46 to 1.72 million in Zhengzhou (CSY, 2007-2014),  
469 which is likely to have resulted in elevated  $NH_3$  emissions. Higher  $NO_2$   
470 concentrations are expected in urban areas due to  $NO_x$  emissions from the combustion  
471 of fossil fuels (Li and Lin, 2000), and also lead to higher  $HNO_3$  concentrations in  
472 urban areas via  $NO_2$  oxidation.

473 The higher  $pNH_4^+$  and  $pNO_3^-$  concentrations observed at urban sites mainly resulted  
474 from the high concentrations at the northern urban sites (NC1~3, NW1 and NW2)  
475 (Fig. 2a and Fig. S2d, e in Supplement). This is probably due to the fact that cities in  
476 northern China, such as Beijing and Zhengzhou in NC and Urumqi in NW, are being  
477 surrounded by intensive agricultural production. Rapid developments along with  
478 urbanization in suburban areas shorten the transport distance between  $NH_3$  emitted  
479 from agriculture and  $SO_2$  and  $NO_x$  emitted from fossil fuel combustion (Gu et al.,  
480 2014). This allows the pollutants to react more readily and form aerosols (e.g.  $PM_{2.5}$ ),  
481 leading to high concentrations of  $pNH_4^+$  and  $pNO_3^-$  near or within cities. This  
482 explanation is supported by the recent MEPC (2013) report that the annual average  
483  $PM_{2.5}$  concentrations in the cities of Beijing, Zhengzhou and Urumqi were more than  
484 twice the Chinese annual mean  $PM_{2.5}$  standard value of  $35 \mu g m^{-3}$ , whereas cities such  
485 as Guangzhou and Xining with little surrounding agricultural production had lower  
486  $PM_{2.5}$  concentrations. In China's 12<sup>th</sup> Five Year Plan (2011–2015), nationwide

删除的内容: the



删除的内容::

488 controls on NO<sub>x</sub> emissions will be implemented along with controls on SO<sub>2</sub> and  
489 primary particle emissions (Wang et al., 2014). In order to better improve the regional  
490 air quality for metropolitan areas, our results suggest that strict control measures on  
491 both NH<sub>3</sub> and NO<sub>x</sub> would be beneficial in NC, at least in the suburban areas.

492 Rural sites in this study also had relatively high concentrations of all measured N<sub>r</sub>  
493 species in air, altogether ranking in the order of NC > NE > NW > SE > SW (Fig. 3f).

494 The higher concentrations in northern China are mainly due to the combined effect of  
495 high NH<sub>3</sub> emissions from N fertilized farmland (Zhang et al., 2008a) and urban air  
496 pollution (e.g. NO<sub>2</sub>, HNO<sub>3</sub>, pNH<sub>4</sub><sup>+</sup> and pNO<sub>3</sub><sup>-</sup>) transported from population centers to  
497 the surrounding rural areas (Luo et al., 2013). The lower air concentrations of N<sub>r</sub>  
498 species at background sites can be ascribed to the lack of both substantial agricultural  
499 and industrial emissions. Additionally, higher wind speeds occurred at some  
500 background areas (e.g. NC12, NC13 and NW4) (Table S1, Supplement), favoring the  
501 dispersion of atmospheric pollutants.

502 We found that regional variations in N<sub>r</sub> concentrations in precipitation were not fully  
503 in accordance with ambient N<sub>r</sub> concentrations (see Sect. 3.2) when assessed by land  
504 use types. It is commonly accepted that N concentrations in precipitation are affected  
505 by the amount of precipitation (Yu et al., 2011). Negative correlations between  
506 precipitation amount and monthly volume-weighted concentrations of NH<sub>4</sub><sup>+</sup>-N and  
507 NO<sub>3</sub><sup>-</sup>-N were obtained by fitting exponential models in all six regions (Fig. S4,  
508 Supplement), indicating a dilution effect of rainwater on inorganic N concentration.  
509 The relationships were not significant ( $p > 0.05$ ) in NW and TP, which is probably  
510 caused by low precipitation amounts at or near the sampling sites (Fig. S5,  
511 Supplement). Nevertheless, dilution could explain some of the regional differences in  
512 precipitation N concentrations.

#### 513 4.2 Dry and wet/bulk deposition of N<sub>r</sub> species

514 A significant ( $p < 0.001$ ) positive correlation was observed between annual dry N  
515 deposition and total annual concentrations of atmospheric N<sub>r</sub> species across all sites  
516 (Fig. S6, Supplement). Therefore, higher concentrations of N<sub>r</sub> species at urban sites  
517 led to higher dry deposition rates compared with rural and background sites, mainly  
518 attributable to elevated N<sub>r</sub> emissions from urban sources (e.g., non-agricultural NH<sub>3</sub>  
519 emissions from landfills, wastewater treatments and NO<sub>x</sub> emissions from traffic  
520 vehicles and power plants) and rapid development of intensive agricultural production  
521 in suburban areas surrounding cities, regardless of differences in dry deposition

删除的内容::



524 velocities of various  $N_r$  species in different land use types. At the national scale, dry N  
525 deposition rates contributed almost half (23-83%, averaging 52%) of the total  
526 inorganic N deposition, indicating the importance of dry deposition monitoring for  
527 comprehensive N deposition quantification.

528 In this study, regional variations of annual wet/bulk N deposition fluxes of  $NH_4^+$ -N,  
529  $NO_3^-$ -N and their sum showed different spatial patterns to those of corresponding  
530 annual VWM concentrations of them in precipitation (see Sect. 3.4). These findings,  
531 together with no significant differences ( $p>0.05$ ) in total annual wet/bulk N deposition  
532 between NC and SE, reflect, not surprisingly, that regional wet/bulk N deposition is  
533 dependent not only on  $N_r$  concentrations in precipitation but also on annual rainfall  
534 amounts. As shown in Fig. 8, annual wet/bulk deposition fluxes of  $NH_4^+$ -N and  
535  $NO_3^-$ -N both showed significantly positive correlations with the corresponding annual  
536 VWM concentrations of inorganic N and annual precipitation amount, especially for  
537  $NH_4^+$ -N, that more significant was found for precipitation amount than concentration.  
538 The measured wet/bulk N deposition rates (average  $19.3 \text{ kg N ha}^{-1} \text{ yr}^{-1}$ ) were almost  
539 twice the earlier average wet deposition value of  $9.9 \text{ kg N ha}^{-1} \text{ yr}^{-1}$  for period of  
540 1990-2003 in China (Lü and Tian, 2007). Our results show similar regional patterns  
541 and comparable magnitudes to those measured in the 2000s in China as reported by  
542 Jia et al. (2014) ( $\sim 14 \text{ kg N ha}^{-1} \text{ yr}^{-1}$ , wet deposition) and Liu et al. (2013) ( $\sim 21 \text{ kg N}$   
543  $\text{ha}^{-1} \text{ yr}^{-1}$ , bulk deposition).

544 The  $NH_4^+$ -N/ $NO_3^-$ -N ratio in wet/bulk deposition can be used to indicate the relative  
545 contribution of  $N_r$  from agricultural and industrial activities to N deposition (Pan et al.,  
546 2012; Zhan et al., 2015; Zhu et al., 2015) because the major anthropogenic source of  
547  $NH_4^+$ -N in precipitation is  $NH_3$  volatilized from animal excrement and the application  
548 of nitrogenous fertilizers in agriculture, while anthropogenic sources of  $NO_3^-$ -N in  
549 precipitation originate from  $NO_x$  emitted from fossil fuel combustion in transportation,  
550 power plant and factories (Cui et al., 2014). In this study the overall annual average  
551 ratio of  $NH_4^+$ -N/ $NO_3^-$ -N in wet/bulk deposition was  $1.3 \pm 0.5$  (standard deviation),  
552 with an increasing (but not significant) trend for urban ( $1.2 \pm 0.6$ ), rural ( $1.3 \pm 0.4$ ),  
553 and background ( $1.5 \pm 0.4$ ) sites (Fig. 5b). Our measured ratio was slightly lower than  
554 average values of 1.6 in Europe (Holland et al., 2005) and 1.5 in the United States (Du  
555 et al., 2014), and similar to an average value (1.2) reported elsewhere for 2013 in  
556 China (Zhu et al., 2015). Based on these findings, we conclude that  $NH_4^+$ -N from  
557 agricultural sources still dominates wet/bulk N deposition but the contribution has

558 decreased drastically between the 1980s and the 2000s (Liu et al., 2013). Reduced N  
559 also contributed more than oxidized N to the total N deposition, and the ratio of  
560 reduced to oxidized N deposition overall averaged  $1.6 \pm 0.7$  in dry deposition and  $1.4$   
561  $\pm 0.4$  in the total deposition (Fig. 5a, c).

562 The overall mean annual deposition fluxes (wet/bulk plus dry) of  $\text{NH}_x$  and  $\text{NO}_y$  for  
563 the period 2010-2014 was graded into five levels and plotted on maps showing the  
564 spatial distribution of  $\text{NH}_3$  and  $\text{NO}_x$  emissions (Fig. 9a, b). The anthropogenic  
565 emission data of  $\text{NH}_3$  and  $\text{NO}_x$  for the year 2010 in China were obtained from  
566 the GAINS (Greenhouse Gas and Air Pollution Interactions and Synergies) model  
567 (<http://www.iiasa.ac.at/>), and emission details for the 33 provinces of China are  
568 summarized in Table S5 of the Supplement. The spatial patterns of estimated  $\text{NH}_x$   
569 and  $\text{NO}_y$  deposition compare reasonably well with the regional patterns of  $\text{NH}_3$  and  
570  $\text{NO}_x$  emissions, respectively, even though the emission data were estimated at the  
571 province scale. With emission data, N deposition can be used to distinguish regional  
572 differences in reactive  $\text{N}_r$  pollution. Across six regions, significantly positive  
573 correlations were found between  $\text{NH}_3$  emissions and  $\text{NH}_x$  deposition fluxes  
574 ( $R^2=0.888$ ,  $p<0.01$ ) (Fig. 9c), and between  $\text{NO}_x$  emissions and  $\text{NO}_y$  deposition fluxes  
575 ( $R^2=0.805$ ,  $p<0.05$ ) (Fig. 9d), implying that the N deposition fluxes to the six regions  
576 are strongly dependent on the spatial pattern of anthropogenic  $\text{N}_r$  emissions among  
577 the regions. The slopes of the relationships of  $\text{NH}_x$  vs.  $\text{NH}_3$ , and  $\text{NO}_y$  vs.  $\text{NO}_x$  were  
578 0.51 and 0.48, which could be roughly interpreted that  $\text{NH}_x$  and  $\text{NO}_y$  deposition  
579 fluxes represent about 51%  $\text{NH}_3$  and 48%  $\text{NO}_x$  emissions, respectively.

580 For all Chinese regions except NC we cannot compare our data with other studies  
581 because observations for different pollution climate sites in other regions are lacking.  
582 For NC, the overall average total N deposition was  $56.2 \pm 14.8 \text{ kg N ha}^{-1} \text{ yr}^{-1}$ , 13-32%  
583 lower than the previously estimated values in Northern China (Pan et al., 2012; Luo et  
584 al., 2013). This difference may reflect differences in the numbers of sampling sites,  
585 land use type and assumed dry deposition velocities. As expected, our estimated  
586 deposition was substantially higher than the results of Lü and Tian (2007), who  
587 suggested that the total N deposition ranged from 13 to 20  $\text{kg N ha}^{-1} \text{ yr}^{-1}$  in NC. This  
588 is attributed to their omission of many major species (e.g., gaseous  $\text{NH}_3$ ,  $\text{HNO}_3$  and  
589 particulate  $\text{N}_r$ ) from their data.

590 Compared to dry and wet N deposition fluxes estimated by CASTNET in the United  
591 States, EMEP in Europe, and EANET sites in Japan, the average values of dry and

592 wet/bulk deposition in China are much higher (**Table 1**). In addition, on the basis of  
593 2001 ensemble-mean modeling results from 21 global chemical transport models (Vet  
594 et al., 2014), three global N deposition hotspots were: western Europe (with levels  
595 from 20.0 to 28.1 kg N ha<sup>-1</sup> yr<sup>-1</sup>), South Asia (Pakistan, India and Bangladesh) from  
596 20.0 to 30.6 kg N ha<sup>-1</sup> yr<sup>-1</sup> and East Asia from 20 to 38.6 kg N ha<sup>-1</sup> yr<sup>-1</sup> in eastern  
597 China (the global maximum). Extensive areas of high deposition from 10 to 20 kg N  
598 ha<sup>-1</sup> yr<sup>-1</sup> appear in the eastern U.S. and southeastern Canada as well as most of central  
599 Europe. Small areas with total deposition of N from 10 to 20 kg N ha<sup>-1</sup> yr<sup>-1</sup> are present,  
600 and very large areas of the continents have deposition from 2 to 10 kg N ha<sup>-1</sup> yr<sup>-1</sup>. In  
601 contrast, the present study shows a much higher total deposition flux (39.9 kg N  
602 ha<sup>-1</sup> yr<sup>-1</sup>) at a national scale. In China, the consumption rates of chemical fertilizer and  
603 fossil fuel have increased 2.0- and 3.2-fold, respectively, between the 1980s and the  
604 2000s (Liu et al., 2013). As a result, the estimated total emission of NH<sub>3</sub> reached 9.8  
605 Tg in 2006, contributing approximately 15% and 35% to the global and Asian NH<sub>3</sub>  
606 emissions (Huang et al., 2012), and NO<sub>x</sub> emissions from fossil fuel combustion  
607 increased from 1.1 Tg N in 1980 to about 6.0 Tg N in 2010 (Liu et al., 2013). The  
608 increasing NO<sub>x</sub> and NH<sub>3</sub> emissions in China led to higher atmospheric N deposition  
609 than those observed in other regions.

610 According to Endo et al. (2011), the low dry deposition fluxes in CASTNET, EMEP  
611 and Japan's EANET network are due at least partly to low concentrations of N<sub>r</sub>  
612 compounds and/or the omission of dry deposition fluxes of major N<sub>r</sub> species (e.g.,  
613 NO<sub>2</sub> and NH<sub>3</sub>) from the data. Meanwhile, the low wet deposition fluxes at these  
614 networks are likely to be a result of the combined effects of low amounts of  
615 precipitation and, especially, low atmospheric N<sub>r</sub> concentrations. In addition,  
616 emissions of nitrogen compounds in other parts of the world are declining. In the U.S.,  
617 for example, NO<sub>x</sub> emissions from the power sector and mobile sources were reduced  
618 by half from 1990 to 2010 (Xing et al., 2013), which explained the declined N  
619 deposition fluxes during the period of 1990-2009 observed at 34 paired dry and wet  
620 monitoring sites in the eastern US (Sickles II et al., 2015). In Europe, the total NO<sub>x</sub>  
621 and NH<sub>3</sub> emissions decreased by 31% and 29% from 1990 to 2009 (Torseth et al.,  
622 2012). N deposition has decreased or stabilized in the United States and Europe since  
623 the late 1980s or early 1990s with the implementation of stricter legislation to reduce  
624 emissions (Goulding et al., 1998; Holland et al., 2005). However, wet deposition of  
625 ammonia or ammonium, which is not regulated, has increased over recent decades in

删除的内容: regions of the globe  
where total deposition is very high

删除的内容: .

删除的内容: .

删除的内容: in

删除的内容: year

632 the U.S. (Du et al., 2014).

### 633 *4.3 Implications of monitoring $N_r$ concentration and deposition on regional N* 634 *deposition simulation*

635 Our results show that atmospheric concentrations and deposition of  $N_r$  in China were  
636 high in the 2000s, although the government has made considerable efforts to control  
637 environmental pollution by improving air quality in mega cities during and after the  
638 2008 Beijing Summer Olympic Games (Wang et al., 2010; Chan and Yao, 2008).  
639 Ideally, the spatial distribution of monitoring sites should reflect the gradients in the  
640 concentrations and deposition fluxes of atmospheric  $N_r$  species. Given the fact that the  
641 arithmetic averages used in this study cannot give a completely accurate evaluation of  
642  $N_r$  levels for the regions of China due to the limited numbers of monitoring sites and  
643 land use types, it is important to develop and improve the quantitative methods for  
644 determining N deposition across China.

645 Numerical models are very useful tools to quantify atmospheric N deposition  
646 (including both spatial and temporal variations), but a challenge to the modeling  
647 approaches is that observations to validate the simulated concentrations and  
648 deposition fluxes are often lacking. In our study 43 monitoring sites were selected in a  
649 range of land use types to provide more representative regional information on N  
650 deposition in China. Although those measurements cannot define all aspects of N  
651 deposition across different regions, they add substantially to existing knowledge  
652 concerning the spatial patterns and magnitudes of N deposition. The present  
653 measurements will be useful for better constraining emission inventories and  
654 evaluating simulations from atmospheric chemistry models. In future studies we will  
655 use models (e.g., FRAME, Dore et al., 2012) integrated with measurements from our  
656 monitoring network to fully address the spatial-temporal variations of atmospheric N  
657 deposition and its impacts on natural and semi-natural ecosystems at the  
658 regional/national level.

### 659 *4.4 Uncertainty analysis of the N dry and wet deposition fluxes*

660 The dry deposition fluxes were estimated by combining measured concentrations with  
661 modeled  $V_d$ . As summarized in **Table S4**, our estimates of dry deposition velocities  
662 for different  $N_r$  species are generally consistent with previous studies (e.g., Flechard  
663 et al., 2011; Pan et al., 2012). Some uncertainties may still exist in the inputs for dry  
664 deposition modeling. For example, underlying surface parameters (e.g., surface  
665 roughness length and land type) strongly affect dry deposition through their effect on

删除的内容: ecosystem

删除的内容: ecosystem

删除的内容: atmospheric

删除的内容: atmospheric

删除的内容: the estimates in

671 both deposition velocity and the absorbability of the ground surface to each of the  
672 gaseous and particulate  $N_r$  species (Loubet et al., 2008). In addition, there is  
673 uncertainty in the deposition fluxes for both  $pNH_4^+$  and  $pNO_3^-$  in our network,  
674 resulting from the difference between the cut-off sizes of particles in the samplers and  
675 that defined in the modeled  $V_d$  which was calculated for atmospheric  $PM_{2.5}$  in  
676 GEOS-Chem model. For example, the cut-off sizes of the samples can collect also  
677 coarse  $NO_3^-$  particles (e.g. calcium nitrate) but should have little effect on  $NH_4^+$   
678 particles (mainly in the fine scale  $<1\text{-}\mu\text{m}$ ) (Tang et al., 2009), resulting in an  
679 underestimation of  $pNO_3^-$  deposition. Furthermore,  $NH_3$  fluxes over vegetated land  
680 are bi-directional and the net direction of this flux is often uncertain. A so-called  
681 canopy compensation point was used in previous studies (Sutton et al., 1998) to  
682 determine the direction of the  $NH_3$  flux. Since the principle of bi-directional  $NH_3$   
683 exchange was not considered in this study,  $NH_3$  deposition may be overestimated at  
684 rural sites with relatively high canopy compensation points (e.g. up to  $5\text{ }\mu\text{g N m}^{-3}$ ) due  
685 to fertilized croplands or vegetation (Sutton et al., 1993).

686 On the other hand, the total dry deposition flux in this study may be underestimated  
687 due to omission of the dry-deposited organic N species in our network and missing  
688  $HNO_3$  data at very few sites as noted earlier (see Sect. 2.2). Organic N species have  
689 been found to make an important contribution to the N dry deposition. For example,  
690 PAN accounted for 20% of the daytime, summertime  $NO_y$  ( $NO + NO_2 + HNO_3 +$   
691  $NO_3^- + PAN$ ) dry deposition at a coniferous forest site (Turnipseed et al., 2006).  
692 However, the contribution of PAN and other known atmospheric organic nitrates to  
693 total  $N_r$  inputs must be minor on an annual time scale, as reported by Flechard et al.  
694 (2012). In previous work, dry deposition flux was inferred from atmospheric  $N_r$   
695 concentrations and a literature-based annual mean deposition velocity (Shen et al.,  
696 2009), or reported by Luo et al. (2013) who did not consider the different dry  
697 deposition velocities of various  $N_r$  species among different land use types. Clearly, in  
698 this study we have greatly improved the estimation of dry deposition, but further work  
699 is still required to increase the reliability and accuracy of N dry deposition values.

700 Since wet/bulk deposition was measured directly, the reported fluxes are considered  
701 more accurate than dry deposition fluxes but still some uncertainties exist. On one  
702 hand, the estimated fluxes obtained from the open precipitation samplers contain  
703 contributions from wet plus unquantifiable dry deposition (including both gases and  
704 particles) and therefore likely overestimate actual wet deposition (Cape et al., 2009).

删除的内容: ere

删除的内容: The o

删除的内容: as

删除的内容: contributors

删除的内容: the

710 For example, our previous research showed that annual unquantifiable dry deposition  
711 (the difference between bulk and wet deposition, approx.  $6 \text{ kg N ha}^{-1}$  on average)  
712 accounted for 20% of bulk N deposition based on observations at three rural sites on  
713 the North China Plain (Zhang et al., 2008b). This contribution increased to 39% in  
714 urban areas based on a recent measurement (Zhang et al., 2015). On the other hand,  
715 dissolved organic N compounds, which have been observed to contribute to be around  
716 25-30% of the total dissolved nitrogen in wet deposition around the world (Jickells et  
717 al., 2013) and approximately 28% of the total atmosphere bulk N deposition in China  
718 (Zhang et al., 2012b), were not considered in the present study. Their exclusion here  
719 would contribute to an underestimation of the total wet N deposition.

720 Although the NNDMN is the only long-term national deposition network to monitor  
721 both N wet/bulk and dry deposition in China till now, large areas of the country and  
722 islands do not contain sampling points which may result in missing hotspots or  
723 pristine sites of N deposition. The implementation of an adequate monitoring program  
724 is also difficult at present in some regions (e.g., northwest China and the Tibetan  
725 Plateau). To address this issue, more new monitoring sites, covering regions with both  
726 extremely low and high  $N_r$  emissions, should be set up in the NNDMN in future  
727 work.

## 728 Conclusions

729 In this paper, we systematically reported large spatial variations in annual mean  
730 concentrations ( $1.3\text{-}47.0 \mu\text{g N m}^{-3}$ ), dry ( $1.1$  to  $52.2 \text{ kg N ha}^{-1} \text{ yr}^{-1}$ ), wet/bulk ( $1.5\text{-}32.5$   
731  $\text{kg N ha}^{-1} \text{ yr}^{-1}$ ) and total ( $2.9$  to  $83.3 \text{ kg N ha}^{-1} \text{ yr}^{-1}$ ) deposition fluxes of atmospheric  
732  $N_r$  species across the forty-three monitoring sites in China. On a regional/national  
733 basis, the annual mean concentrations and deposition fluxes of  $N_r$  species ranked by  
734 the same order of urban > rural > background sites and NC > SE > SW > NE > NW >  
735 TP, reflecting the impact of varying anthropogenic  $N_r$  emissions in different land use  
736 types and/or regions.

737 Dry deposition fluxes of  $N_r$  species on average contributed 52% of the total N  
738 deposition ( $39.9 \text{ kg N ha}^{-1} \text{ yr}^{-1}$ ) across all sites, indicating the importance of dry  
739 deposition monitoring for a complete N deposition assessment at the national scale.  
740 Annual average ratios of reduced N/oxidized N in dry, wet/bulk and total deposition  
741 were 1.6, 1.3 and 1.4, respectively, suggesting that reduced N, mainly from

删除的内容: or

删除的内容: lack of

删除的内容: be

745 agricultural sources, still dominates dry, wet/bulk, and total N deposition in China.  
746 Our work represents the first effort to investigate both dry and wet/bulk N deposition  
747 simultaneously, based on a nationwide monitoring network in China. We consider this  
748 unique dataset important not only for informing policy-makers about the abatement of  
749 pollutant emissions and ecosystem protection but also validating model estimations of  
750 N deposition at the regional/national scale. For better understanding atmospheric N  
751 deposition fluxes in China, further studies in the future are still required at least the  
752 two following aspects: (1) to cover more representative monitoring sites; (2) to  
753 improve the dry deposition velocity estimates of various  $N_r$  species using a  
754 single-point dry deposition model as for CASTNET.

### 755 **Acknowledgments**

756 This study was supported by the Chinese National Basic Research Program  
757 (2014CB954202), the China Funds for Distinguished Young Scholars of NSFC  
758 (40425007), and the National Natural Science Foundation of China (31121062,  
759 41321064 and 41405144). The authors thank all technicians at monitoring sites in  
760 NNDMN.

### 762 **References**

- 763 Bey, I., Jacob, D. J., Yantosca, R. M., Logan, J. A., Field, B. D., Fiore, A. M., Li, Q.,  
764 Liu, H., Mickley, L. J., and Schultz, M. G.: Global modeling of tropospheric  
765 chemistry with assimilated meteorology: Model description and evaluation, J.  
766 Geophys. Res., 106(D19), 23,073 –23,096, 2001.
- 767 Behera, S. N., Sharma, M., Aneja, V. P., and Balasubramanian, R.: Ammonia in the  
768 atmosphere: a review on emission sources, atmospheric chemistry and deposition  
769 on terrestrial bodies, Environ. Sci. Pollut. Res., 20, 8092–8131,  
770 doi:10.1007/s11356-013-2051-9, 2013.
- 771 Cape, J.N., Van Dijk, N., and Tang, Y.S.: Measurement of dry deposition to bulk  
772 collectors using a novel flushing sampler. J. Environ. Monit., 11, 353-358,  
773 doi: 10.1039/B813812E, 2009.
- 774 Chan, C.K. and Yao, X.H.: Air pollution in mega cities in China, Atmos. Environ., 42,

已下移 [3]: Our study represents the first effort to investigate inorganic dry and wet/bulk N deposition simultaneously, based on a nationwide monitoring network in China.

删除的内容: Our study represents the first effort to investigate inorganic dry and wet/bulk N deposition simultaneously, based on a nationwide monitoring network in China. We ...

已下移 [1]: We consider this unique dataset important not only for informing policy-makers about the abatement of pollutant emissions and ecosystem protection but also to validate model estimations of N deposition at the regional/national scale in China.

带格式的: 字体: (默认) Times New Roman, (中文) +中文正文, 小四

已下移 [2]: Dry N deposition correlated well with total concentrations of  $N_r$  in the air, but differences were found between patterns of wet/bulk N deposition and the  $N_r$  concentration in precipitation. This reflects the combining effect of both  $N_r$  concentrations and precipitation amounts on regional wet/bulk N deposition.

已移动(插入) [2]

已移动(插入) [3]

已移动(插入) [1]

带格式的: 字体: Times New Roman, 小四

带格式的: 字体: Times New Roman, 小四



803 1–42, doi: 10.1016/j.atmosenv.2007.09.003, 2008.

804 Chen, D., Wang, Y. X., McElroy, M. B., He, K., Yantosca, R. M., and Le Sager, P.:  
805 Regional CO pollution in China simulated by high-resolution nested-grid  
806 GEOS-Chem model, *Atmos. Chem. Phys.*, 11, 3825-3839, 2009.

807 Chen, X. Y. and Mulder, J.: Atmospheric deposition of nitrogen at five subtropical  
808 forested sites in South China, *Sci. Total Environ.*, 378, 317–330, doi:  
809 10.1016/j.scitotenv.2007.02.028, 2007.

810 Clark, C. M. and Tilman, D.: Loss of plant species after chronic low-level nitrogen  
811 deposition to prairie grasslands, *Nature*, 451, 712–715, doi:10.1038/nature06503,  
812 2008.

813 Clarke, J. F., Edgerton, E. S., and Martin, B. E.: Dry deposition calculations for the  
814 Clean Air Status and Trends Network, *Atmos. Environ.*, 31, 3667-3678, 1997.

815 CSY (China Statistical Yearbook), 2007-2014. Available at: <http://www.stats.gov.cn>.

816 Cui, J., Zhou, J., Peng, Y., He, Y. Q., Yang, H., Mao, J. D., Zhang, M. L., Wang, Y. H.,  
817 and Wang, S. W.: Atmospheric wet deposition of nitrogen and sulfur in the  
818 agroecosystem in developing and developed areas of Southeastern China, *Atmos.*  
819 *Environ.*, 89, 102–108, doi:10.1016/j.atmosenv.2014.02.007, 2014.

820 Dentener, F., Drevet, J., Lamarque, J. F., Bey, L., Eickhout, B., Fiore, A.  
821 M. Hauglustaine, D., Horowitz, L. W., Krol, M., and Kulshrestha, U. C. :  
822 Nitrogen and sulfur deposition on regional and global scales: a multimodel  
823 evaluation, *Global Biogeochemical Cy.*, 20, GB4003, doi: 10.1029/2005GB002672,  
824 2006.

825 Dore, A.J., Kryza, M., Hall, J. Hallsworth, S., Keller, V., Vieno, M. and Sutton, M.A.:  
826 The influence of model grid resolution on estimation of national scale nitrogen  
827 deposition and exceedance of critical loads, *Biogeosciences*, 9, 1597-1609, 2012.

828 Du, E. Z., Vries, W. D., Galloway, J. N., Hu, X. Y., and Fang, J. Y.: Changes in wet  
829 nitrogen deposition in the United States between 1985 and 2012, *Environ. Res.*  
830 *Lett.*, 9, 095004, doi:10.1088/1748-9326/9/9/095004, 2014.

831 EEA: Air Quality in Europe-2011 Report. Technical Report 12/2011. EEA,  
832 Copenhagen, 2011.



833 Ellis, R. A., Jacob, D. J., Sulprizio, M. P., Zhang, L., Holmes, C. D., Schichtel, B. A.,  
834 Blett, T., Porter, E., Pardo, L. H., and Lynch, J. A.: Present and future nitrogen  
835 deposition to national parks in the United States: critical load exceedances, *Atmos.*  
836 *Chem. Phys.*, 13, 9083-9095, doi:10.5194/acp-13-9083-2013, 2013.

837 Endo, T., Yagoh, H., Sato, K., Matsuda, K., Hayashi, K., Noguchi, I., and Sawada, K.:  
838 Regional characteristics of dry deposition of sulfur and nitrogen compounds at  
839 EANET sites in Japan from 2003 to 2008, *Atmos. Environ.*, 45,  
840 1259–1267, doi:10.1016/j.atmosenv.2010.12.003, 2010.

841 Erismann, J. W., Vermeulen, A., Hensen, A., Flechard, C., Dammggen, U., Fowler, D.,  
842 Sutton, M., Grunhage, L., and Tuovinen, J.P.: Monitoring and modelling of  
843 biosphere/atmosphere exchange of gases and aerosols in Europe, *Environ. Pollut.*,  
844 133, 403–413, doi:10.1016/j.envpol.2004.07.004, 2005.

845 Flechard, C. R., Nemitz, E., Smith, R. I., Fowler, D., Vermeulen, A. T., Bleeker, A.,  
846 Erismann, J. W., Simpson, D., Zhang, L., Tang, Y. S., and Sutton, M. A.: Dry  
847 deposition of reactive nitrogen to European ecosystems: a comparison of inferential  
848 models across the NitroEurope network, *Atmos. Chem. Phys.*, 11,  
849 2703–2728, doi:10.5194/acp-11-2703-2011, 2011.

850 Fowler, D., Coyle, M., Skiba, U., Sutton, M. A., Cape, J. N., Reis, S., Sheppard, L. J.,  
851 Jenkins, A., Grizzetti, B., Galloway, J. N., Vitousek, P., Leach, A., Bouwman, A. F.,  
852 Butterbach-Bahl, K., Dentener, F., Stevenson, D., Amann, M., and Voss, M.: The  
853 global nitrogen cycle in the twenty-first century, *Phil. Trans. R. Soc. B*, 368,  
854 20130164, doi:10.1098/rstb.2013.0164, 2013.

855 Galloway, J. N., Dentener, F. J., Capone, D. G., Boyer, E. W., Howarth, R. W.,  
856 Seitzinger, S. P., Asner, G. P., Cleveland, C. C., Green, P. A., Holland, E. A., Karl,  
857 D. M., Michaels, A. F., Porter, J. H., Townsend, A. R., and Vorosmarty, C. J.:  
858 Nitrogen cycles: past, present, and future, *Biogeochem.*, 70, 153–226, 2004.

859 Galloway, J. N., Townsend, A. R., Erismann, J. W., Bekunda, M., Cai, Z., Frenney, J. R.,  
860 Martinelli, L. A., Seitzinger, S. P., and Sutton, M. A.: Transformation of the  
861 Nitrogen Cycle: Recent trends, questions, and potential solutions, *Science*, 320,  
862 889–892, 2008.

863 Galloway, J. N., Leach, A. M., Bleeker, A., and Erisman, J. W.: A chronology of  
864 human understanding of the nitrogen cycle, *Phil. Trans. R. Soc. B*, 368, 20130120,  
865 doi:10.1098/rstb.2013.0120, 2013.

866 Goulding, K. W. T., Bailey, N. J., Bradbury, N. J., Hargreaves, P., Howe, M., Murphy,  
867 D. V., Poulton, P. R., and Willison, T. W.: Nitrogen deposition and its contribution  
868 to nitrogen cycling and associated soil processes, *New Phytol.*, 139, 49–58, 1998.

869 Gu, B. J., Ge, Y., Ren, Y., Xu, B., Luo, W. D., Jiang, H., Gu, B. H., and Chang, J.:  
870 Atmospheric reactive nitrogen in China: Sources, recent trends, and damage costs,  
871 *Environ. Sci. Technol.*, 46, 9240–9247, doi:10.1021/es301446g, 2012.

872 Gu, B. J., Sutton, M. A., Chang, S. X., Ge, Y., and Jie, C.: Agricultural ammonia  
873 emissions contribute to China's urban air pollution, *Front. Ecol. Environ.*, 12,  
874 265–266, doi:10.1890/14.WB.007, 2014.

875 Holland, E. A., Braswell, B. H., Sulzman, J., and Lamarque, J. F.: Nitrogen deposition  
876 onto the United States and Western Europe: synthesis of observations and models,  
877 *Ecol. Appl.*, 15, 38–57, 2005.

878 Hu, H., Yang, Q., Lu, X., Wang, W., Wang, S., and Fan, M.: Air pollution and control  
879 in different areas of China. *Crit. Rev. Environ. Sci. Technol.*, 40, 452–518,  
880 doi:10.1080/10643380802451946, 2010.

881 Huang, X., Song, Y., Li, M. M., Li, J. F., Huo, Q., Cai, X. H., Zhu, T., Hu, M., and  
882 Zhang, H. S.: A high-resolution ammonia emission inventory in China, *Global*  
883 *Biogeochem. Cy.*, 26, GB1030, doi:10.1029/2011GB004161, 2012.

884 Huang, Y. L., Lu, X. X., and Chen, K.: Wet atmospheric deposition of nitrogen: 20  
885 years measurement in Shenzhen City, China, *Environ. Monit. Assess.*, 185, 113–  
886 122, doi: 10.1007/s10661-012-2537-9, 2013.

887 Jia, Y. L., Yu, G. R., He, N. P., Zhan, X. Y., Fang, H. J., Sheng, W. P., Zuo, Y., Zhang,  
888 D. Y., and Wang, Q. F.: Spatial and decadal variations in inorganic nitrogen wet  
889 deposition in China induced by human activity. *Sci. Rep.*, 4, 3763, doi:  
890 10.1038/srep03763, 2014.

891 Jickells, T., Baker, A. R., Cape, J. N., Cornell, S.E., and Nemitz, E.: The cycling of  
892 organic nitrogen through the atmosphere. *Philos. Trans. R. Soc. B* 368, 20130115,

893 doi:org/10.1098/rstb.2013.0115, 2013.

894 Li, Y. E. and Lin, E. D.: Emissions of N<sub>2</sub>O, NH<sub>3</sub> and NO<sub>x</sub> from fuel combustion,  
895 industrial processes and the agricultural sectors in China. *Nutr. Cycl. Agroecosys.*,  
896 57, 99–106, 2000.

897 Liu, X. J., Song, L., He, C. E., and Zhang, F. S.: Nitrogen deposition as an important  
898 nutrient from the environment and its impact on ecosystems in China, *J. Arid Land*,  
899 2, 137–143, 2010.

900 Liu, X. J., Duan, L., Mo, J. M., Du, E., Shen, J. L., Lu, X. K., Zhang, Y., Zhou, X. B.,  
901 He, C. E., and Zhang, F. S.: Nitrogen deposition and its ecological impact in China:  
902 An overview, *Environ. Pollut.*, 159, 2251–2264, doi:10.1016/j.envpol.2010.08.002,  
903 2011.

904 Liu, X. J., Zhang, Y., Han, W. X., Tang, A., Shen, J. L., Cui, Z. L., Vitousek, P.,  
905 Erisman, J. W., Goulding, K., Christie, P., Fangmeier, A., and Zhang, F. S.:  
906 Enhanced nitrogen deposition over China, *Nature*, 494, 459–462,  
907 doi:10.1038/nature11917, 2013.

908 Liu, X. J., Xu, W., Pan, Y. P., and Du, E. Z.: Liu et al. suspect that Zhu et al. (2015)  
909 may have underestimated dissolved organic nitrogen (N) but overestimated total  
910 particulate N in wet deposition in China, *Sci. Total Environ.*, 520, 300–301,  
911 doi.org/10.1016/j.scitotenv.2015.03.004, 2015.

912 Loubet, B., Asman, W. A. H., Theobald, M. R., Hertel, O., Tang, S. Y., Robin, P.,  
913 Hassouna, M., Dämmgen, U., Genermont, S., Cellier, P., and Sutton, M. A.:  
914 Ammonia deposition near hot spots: processes, models and monitoring methods. In:  
915 Sutton MA, Reis S, Baker SMH, editors. *Atmospheric ammonia: detecting  
916 emission changes and environmental impacts*. Netherlands: Springer;  
917 205-251.,2008.

918 Lü, C. Q. and Tian, H. Q.: Spatial and temporal patterns of nitrogen deposition in  
919 China: Synthesis of observational data, *J. Geophys. Res.*, 112, D22S05,  
920 doi:10.1029/2006JD007990, 2007.

921 Lü, C. Q. and Tian, H. Q.: Half-century nitrogen deposition increase across China: A  
922 gridded time-series data set for regional environmental assessments. *Atmos.*

923 Environ., 97, 68-74, 2014.

924 Luo, X. S., Liu, P., Tang, A. H., Liu, J. Y., Zong, X. Y., Zhang, Q., Kou, C. L., Zhang,  
925 L. J., Fowler, D., Fangmeier, A., Christie, P., Zhang, F. S., and Liu, X. J.: An  
926 evaluation of atmospheric Nr pollution and deposition in North China after the  
927 Beijing Olympics, Atmos. Environ., 74, 209–216,  
928 doi:10.1016/j.atmosenv.2013.03.054, 2013.

929 Maston, P., Lohse, K. A., and Hall, S. J.: The globalization of nitrogen deposition:  
930 Consequences for terrestrial ecosystems, *Ambio*, 31, 113–119, 2002.

931 MEPC (Ministry of Environmental Protection of the People’s Republic of China):  
932 China’s environment and data center. [www.zhb.gov.cn/](http://www.zhb.gov.cn/). Viewed 23 April 2014,  
933 2014

934 Pan, Y. P., Wang, Y. S., Tang, G. Q., and Wu, D.: Wet and dry deposition of  
935 atmospheric nitrogen at ten sites in Northern China. *Atmos. Chem. Phys.*, 12,  
936 6515-6535, doi:10.5194/acp-12-6515-2012, 2012.

937 Reche, C., Viana, M., Pandolfi, M., Alastuey, A., Moreno, T., Amato, F., Ripoll, A.,  
938 and Querol, X.: Urban NH<sub>3</sub> levels and sources in a Mediterranean environment.  
939 *Atmos. Environ.*, 57:153–164, doi:10.1016/j.atmosenv.2012.04.021, 2012.

940 Richter, D. D., Burrows, J. P., N Nüß, H., Granier, C., and Niemeier, U.: Increase in  
941 tropospheric nitrogen dioxide over China observed from space, *Nature* 437,  
942 129–132, 2005.

943 Seinfeld, J. and Pandis, S.: *Atmospheric Chemistry and Physics: From Air Pollution*  
944 *to Climate Change*, John Wiley and Sons, 2<sup>nd</sup> Edition, 1203 pp., 2006.

945 Schwede, D., Zhang, L., Vet, R., and Lear, G.: An intercomparison of the deposition  
946 models used in the CASTNET and CAPMoN networks, *Atmos. Environ.*, 45,  
947 1337–1346, doi:10.1016/j.atmosenv.2010.11.050, 2011.

948 Shen, J. L., Tang, A. H., Liu, X. J., Fangmeier, A., Goulding, K. T. W., and Zhang, F.  
949 S.: High concentrations and dry deposition of reactive nitrogen species at two sites  
950 in the North China Plain, *Environ. Pollut.*, 157, 3106–3113,  
951 doi:10.1016/j.envpol.2009.05.016, 2009.

952 Simpson, D., Fagerli, H., Jonson, J.E., Tsyro, S., Wind, P., and Tuovinen, J. P.:

953 Trans-boundary Acidification and Eutrophication and Ground Level Ozone in  
954 Europe: Unified EMEP Model Description, EMEP Status Report 1/2003 Part I,  
955 EMEP/MSC-W Report, The Norwegian Meteorological Institute, Oslo, Norway,  
956 2003.

957 Skeffington, R. A. and Hill, T. J.: The effects of a changing pollution climate on  
958 throughfall deposition and cycling in a forested area in southern England, *Sci. Total*  
959 *Environ.*, 434 , 28–38, doi:10.1016/j.scitotenv.2011.12.038, 2012.

960 Sickles, J. E. and Shadwick, D. S.: Air quality and atmospheric deposition in the  
961 eastern US: 20 years of change, *Atmos. Chem. Phys.*, 15, 173–197, doi:  
962 10.5194/acp-15-173-2015, 2015.

963 Sutton, M.A., Pitcairn, C.E.R., and Fowler, D.: The exchange of ammonia between  
964 the atmosphere and plant communities. *Adv. Ecol. Res.*, 24, 301-393,  
965 doi:10.1016/S0065-2504(08)60045-8, 1993.

966 Sutton, M. A., Burkhardt, J. K., Guerin, D., Nemitz, E., and Fowler, D.: Development  
967 of resistance models to describe measurements of bi-directional ammonia  
968 surface-atmosphere exchange, *Atmos. Environ.*, 32, 473–480,  
969 doi:10.1016/S1352-2310(97)00164-7,1998.

970 Sutton, M. A., Tang, Y. S., Miners, B., and Fowler, D.: A new diffusion denuder  
971 system for long-term, regional monitoring of atmospheric ammonia and ammonium,  
972 *Water Air Soil Poll. Focus*, 1, 145–156, 2001.

973 Tang, Y. S., Simmons, I., van Dijk, N., Di Marco, C., Nemitz, E., Dammgén,  
974 U., Gilke, K., Djuricic, V., Vidic, S., Gliha, Z.: European scale application of  
975 atmospheric reactive nitrogen measurements in a low-cost approach to infer dry  
976 deposition fluxes. *Agr. Ecosyst. Environ.*, 133, 183–195, doi:  
977 10.1016/j.agee.2009.04.027, 2009.

978 Torseth, K., Aas, W., Breivik, K., Fjaeraa, A. M., Fiebig, M., Hjellbrekke, A. G.,  
979 Myhre, C. L., Solberg, S., Yttri, K. E.: Introduction to the European Monitoring and  
980 Evaluation Programme (EMEP) and observed atmospheric composition change  
981 during 1972–2009, *Atmos. Chem. Phys.*, 12, 5447–5481, doi:  
982 10.5194/acp-12-5447-2012, 2012.

983 Vitousek, P. M., Aber, J. D., Howarth, R. W., Likens, G. E., Matson, P. A., Schindler,  
984 D. W., Schlesinger, W. H., and Tilman, D. G.: Human alteration of the global  
985 nitrogen cycle: Sources and consequences, *Ecol. Appl.*, 7, 737–750, 1997.

986 Vet, R., Artz, R. S., Carou, S., Shaw, M., Ro, C-U., Aas, W., Baker, A., and 14 authors:  
987 A global assessment of precipitation chemistry and deposition of sulfur, nitrogen,  
988 sea salt, base cations, organic acids, acidity and pH, and phosphorus, *Atmos.*  
989 *Environ.*, 93, 3–100, doi:10.1016/j.atmosenv.2013.10.060, 2014.

990 Wang, S. X., Xing, J., Zhao, B., Jang, C., and Hao, J. M.: Effectiveness of national air  
991 pollution control policies on the air quality in metropolitan areas of China, *J.*  
992 *Environ. Sci.*, 26, 13–22, doi: 10.1016/S1001-0742(13)60381-2, 2014.

993 Wang, T., Nie, W., Gao, J., Xue, L. K., Gao, X. M., Wang, X. F., Qiu, J., Poon, C. N.,  
994 Meinardi, S., Blake, D., Wang, S. L., Ding, A. J., Chai, F. H., Zhang, Q. Z., and  
995 Wang, W. X.: Air quality during the 2008 Beijing Olympics: secondary pollutants  
996 and regional impact, *Atmos. Chem. Phys.*, 16, 7603–7615,  
997 doi:10.5194/acp-10-7603-2010, 2010.

998 Wesely, M. L.: Parameterization of surface resistances to gaseous dry deposition in  
999 regional-scale numerical-models, *Atmos. Environ.*, 23, 1293-1304, 1989.

1000 Xing, J., Pleim, J., Mathur, R., Pouliot, G., Hogrefe, C., Gan, C. M., Wei, C.:  
1001 Historical gaseous and primary aerosol emissions in the United States from 1990 to  
1002 2010, *Atmos. Chem. Phys.*, 13, 7531–7549, doi: 10.5194/acp-13-7531-2013, 2013.

1003 Yu, W. T., Jiang, C. M., Ma, Q., Xu, Y. G., Zou, H., and Zhang, S. C.: Observation of  
1004 the nitrogen deposition in the lower Liaohe River Plain, Northeast China and  
1005 assessing its ecological risk, *Atmos. Res.*, 101, 460–468,  
1006 doi:10.1016/j.atmosres.2011.04.011, 2011.

1007 Zhan, X., Yu, G., He, N., Jia, B., Zhou, M., Wang, C., Zhang, J., Zhao, G., Wang, S.,  
1008 Liu, Y., and Yan, J.: Inorganic nitrogen wet deposition: Evidence from the  
1009 North-South Transect of Eastern China, *Environ. Pollut.*, 204, 1–8, doi:  
1010 10.1016/j.envpol.2015.03.016, 2015.

1011 Zhang, F. S., Wang, J. Q., Zhang, W. F., Cui, Z. L., Ma, W. Q., Chen, X. P., and Jiang,  
1012 R. F.: Nutrient use efficiency of major cereal crops in China and measures for

1013 improvement. Acta. Pedologia Sinica, 45, 915–924, 2008a (in Chinese with English  
1014 abstract).

1015 Zhang, G. Z., Pan, Y. P., Tian, S. L., Cheng, M. T., Xie, Y. Z., Wang, H., and Wang, Y.  
1016 S.: Limitations of passive sampling technique of rainfall chemistry and wet  
1017 deposition flux characterization. Res. Environ. Sci., 28, 684-690, doi:10.  
1018 13198/j.issn.1001-6929.2015.05.03, 2015.

1019 Zhang, L., Jacob, D. J., Knipping, E. M., Kumar, N., Munger, J. W., Carouge, C. C.,  
1020 van Donkelaar, A., Wang, Y. X., and Chen, D.: Nitrogen Deposition to the United  
1021 States: Distribution, Sources, and Processes, Atmos. Chem. Phys., 12, 4539-4554,  
1022 doi:10.5194/acp-12-4539-2012, 2012a.

1023 Zhang, L. M., Gong, S. L., Padro, J., and Barrie, L.: A size-segregated particle dry  
1024 deposition scheme for an atmospheric aerosol module, Atmos. Environ., 35 (3),  
1025 549-560, doi:10.1016/s1352-2310(00)00326-5, 2001.

1026 Zhang, Y., Liu, X. J., Fangmeier, A., Goulding, K. T. W., and Zhang, F. S.: Nitrogen  
1027 inputs and isotopes in precipitation in the North China Plain, Atmos. Environ., 42,  
1028 1436–1448, doi:10.1016/j.atmosenv.2007.11.002, 2008b.

1029 Zhang, Y., Dore, A. J., Ma, L., Liu, X. J., Ma, W. Q., Cape, J. N., and Zhang, F. S.:  
1030 Agricultural ammonia emissions inventory and spatial distribution in the North  
1031 China Plain, Environ. Pollut., 158, 490–501, doi:10.1016/j.envpol.2009.08.033,  
1032 2010.

1033 Zhang, Y., Song, L., Liu, X. J., Li, W. Q., Lü, S. H., Zheng, L. X., Bai, Z. C., Cui,  
1034 G.Y., and Zhang, F. S.: Atmospheric organic nitrogen deposition in China. Atmos.  
1035 Environ., 46, 195–204, doi:10.1016/j.atmosenv.2011.09.080, 2012b.

1036 Zhao, Y. H., Zhang, L., Pan, Y. P., Wang, Y. S., Paulot, F., and Henze, D. K.:  
1037 Atmospheric nitrogen deposition to the northwestern Pacific: seasonal variation and  
1038 source attribution, Atmos. Chem. Phys. Discuss., 15, 13657-13703,  
1039 doi:10.5194/acpd-15-13657-2015, 2015.

1040 Zhu, J. X., He, N. P., Wang, Q. F., Yan, G. F., Wen, D., Yu, G. R., and Jia, Y. L.: The  
1041 composition, spatial patterns, and influencing factors of atmospheric wet nitrogen  
1042 deposition in Chinese terrestrial ecosystems. Sci. Total Environ., 511, 777-785,

已移动(插入) [4]

删除的内容: b

删除的内容: ■

已上移 [4]: Zhang, L., Jacob, D. J.,  
Knipping, E. M., Kumar, N., Munger,  
J. W., Carouge, C. C., van Donkelaar,  
A., Wang, Y. X., and Chen, D.:  
Nitrogen Deposition to the United  
States: Distribution, Sources, and  
Processes, Atmos. Chem. Phys., 12,  
4539-4554,  
doi:10.5194/acp-12-4539-2012,  
2012Zhang, L. M., Gong, S. L., Padro  
J., and Barrie, L.: A size-segregated  
particle dry deposition scheme for an  
atmospheric aerosol module, Atmos.  
Environ., 35 (3), 549-560,  
doi:10.1016/s1352-2310(00)00326-5,  
2001. ■

删除的内容: 2012a

删除的内容: 12

带格式的: 缩进: 左侧: 0 厘米,  
悬挂缩进: 1 字符, 首行缩进: -1  
字符, 到齐到网格

1063 doi.org/10.1016/j.scitotenv.2014.12.038, 2015.

1064 **Figure captions**

1065 **Fig. 1.** Geographical distribution of the forty-three monitoring sites in China.

1066 **Fig. 2.** Annual mean concentrations of  $N_r$  compounds in air (a) and volume-weighted  
1067 concentrations of inorganic nitrogen species in precipitation (b) at all monitoring sites.

1068 U, R, and B denote urban, rural, and background sites, respectively. TP denotes the  
1069 Tibetan Plateau.

1070 **Fig. 3.** Annual mean concentrations of (a)  $NH_3$ ; (b)  $NO_2$ ; (c)  $HNO_3$ ; (d)  $pNH_4^+$ ; (e)  
1071  $pNO_3^-$ ; and (f) Total  $N_r$ : sum of all measured  $N_r$  in air and volume-weighted  
1072 concentrations of  $NH_4^+$  (g);  $NO_3^-$  (h) and Total inorganic N (TIN): sum of  $NH_4^+$  and  
1073  $NO_3^-$  (i) in precipitation at different land use types in six regions. The number of sites  
1074 with the same land use type in each region can be found in Table S1 in the  
1075 Supplement. The error bars are the standard errors of means.

1076 **Fig. 4.** Annual mean concentrations and deposition fluxes of  $N_r$  compounds at  
1077 different land use types across China: concentrations in air (a); volume-weighted  
1078 concentrations in precipitation (b); dry N deposition fluxes (c); wet/bulk N deposition  
1079 fluxes (d). The number of sites with the same land use type can be found in Table S1  
1080 in the Supplement. The error bars are the standard errors of means.

1081 **Fig. 5.** Annual deposition flux of various  $N_r$  species at the forty-three selected sites in  
1082 China: (a) dry deposition flux; (b) wet/bulk deposition flux; (c) total deposition flux.  
1083 Yellow dots denote ratios of reduced N to oxidized N in dry deposition (a),  $NH_4^+$ -N  
1084 to  $NO_3^-$ -N in wet/bulk deposition (b) and/or reduced N to oxidized N in total  
1085 deposition (c) at all sampling sites. U, R, and B denote urban, rural, and background  
1086 sites, respectively. TP denotes the Tibetan Plateau.

1087 **Fig. 6.** Dry N deposition fluxes of (a)  $NH_3$ ; (b)  $NO_2$ ; (c)  $HNO_3$ ; (d)  $pNH_4^+$ ; (e)  $pNO_3^-$ ;  
1088 and (f) Total  $N_r$ : sum of all measured  $N_r$  in dry and wet/bulk N deposition fluxes of  
1089  $NH_4^+$  (g);  $NO_3^-$  (h) and Total inorganic N (TIN): sum of  $NH_4^+$  and  $NO_3^-$  (i) at  
1090 different land use types in the six regions. The number of sites with the same land use  
1091 type in each region can be found in Table S1 in the Supplement. Error bars are  
1092 standard errors of means.

带格式的: 字体颜色: 自动设置

删除的内容: Error

带格式的: 字体颜色: 自动设置

带格式的: 字体: 非加粗



1094 **Fig. 7.** Contribution of different pathways (dry-deposited N=gaseous N+ particulate N,  
1095 wet/bulk-deposited N=precipitation N) to the estimated total N deposition in the six  
1096 regions: (a) NC: north China; (b) NE: northeast China; (c) NW: northwest China; (d)  
1097 SE: southeast China; (e) SW: southwest China; (f) TP: Tibetan Plateau.

1098 **Fig. 8.** Correlations between annual wet/bulk  $\text{NH}_4^+$ -N deposition and annual  
1099 volume-weighted concentration of  $\text{NH}_4^+$ -N (a) and annual precipitation (b); between  
1100 annual wet/bulk  $\text{NO}_3^-$ -N deposition and annual volume-weighted concentration of  
1101  $\text{NO}_3^-$ -N (c) and annual precipitation (d).

1102 **Fig. 9.** Spatial variation of atmospheric N deposition flux with emission distribution  
1103 in China: (a)  $\text{NH}_3$  emission vs.  $\text{NH}_x$  deposition; (b)  $\text{NO}_x$  emission vs.  $\text{NO}_y$  deposition;  
1104 (c) relationship of  $\text{NH}_x$  deposition vs.  $\text{NH}_3$  emission; (d) relationship of  $\text{NO}_y$   
1105 deposition vs.  $\text{NO}_x$  emission.

1106

1107

1108

1109

1110

1111

1112

1113

1114

1115

1116

1117

1118

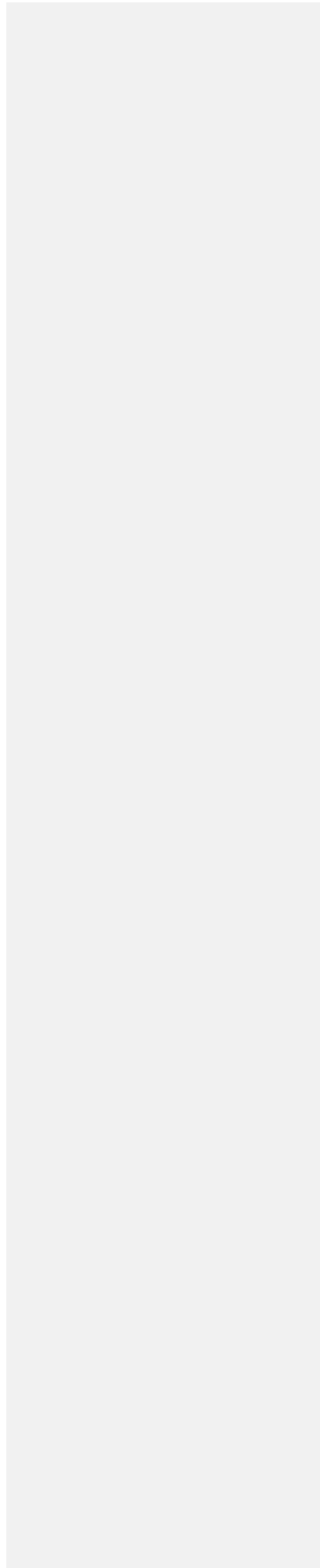
1119

1120

1121

1122

1123

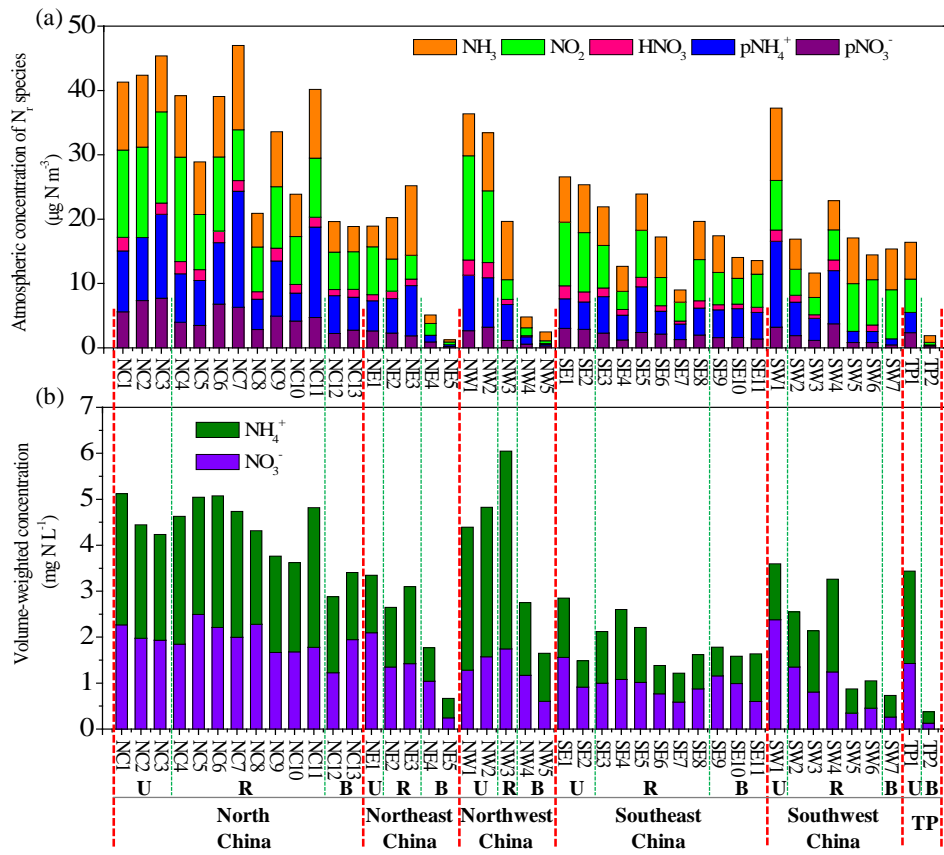


1125 **Figure 1**



1127

**Figure 2**



1128

1129

1130

1131

1132

1133

1134

1135

1136

1137

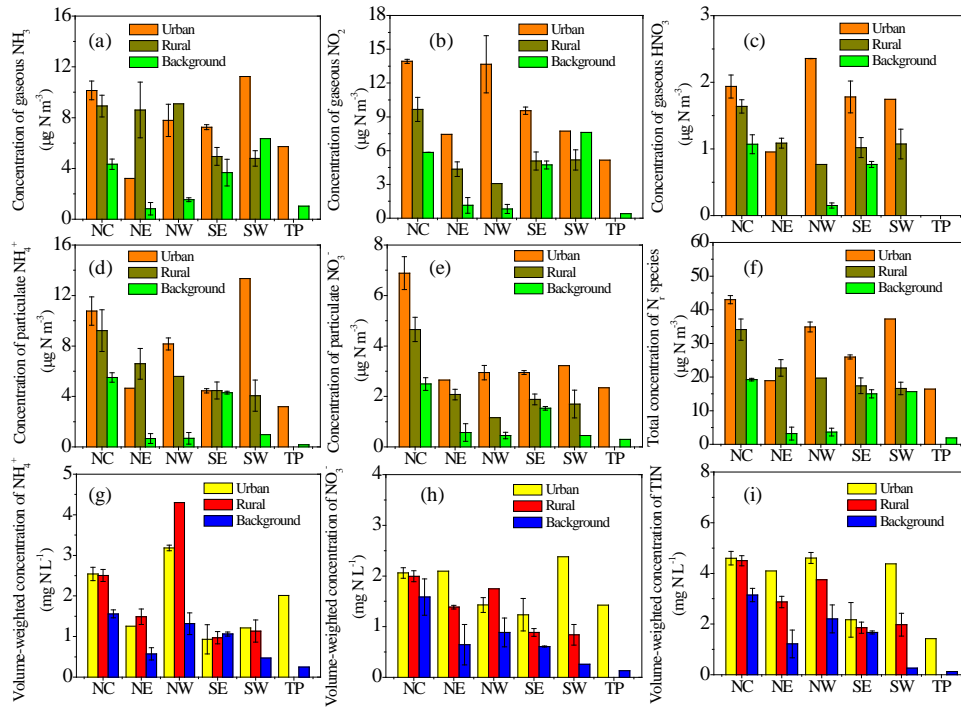
1138

1139

1140

1141

1142 **Figure 3**



1143

1144

1145

1146

1147

1148

1149

1150

1151

1152

1153

1154

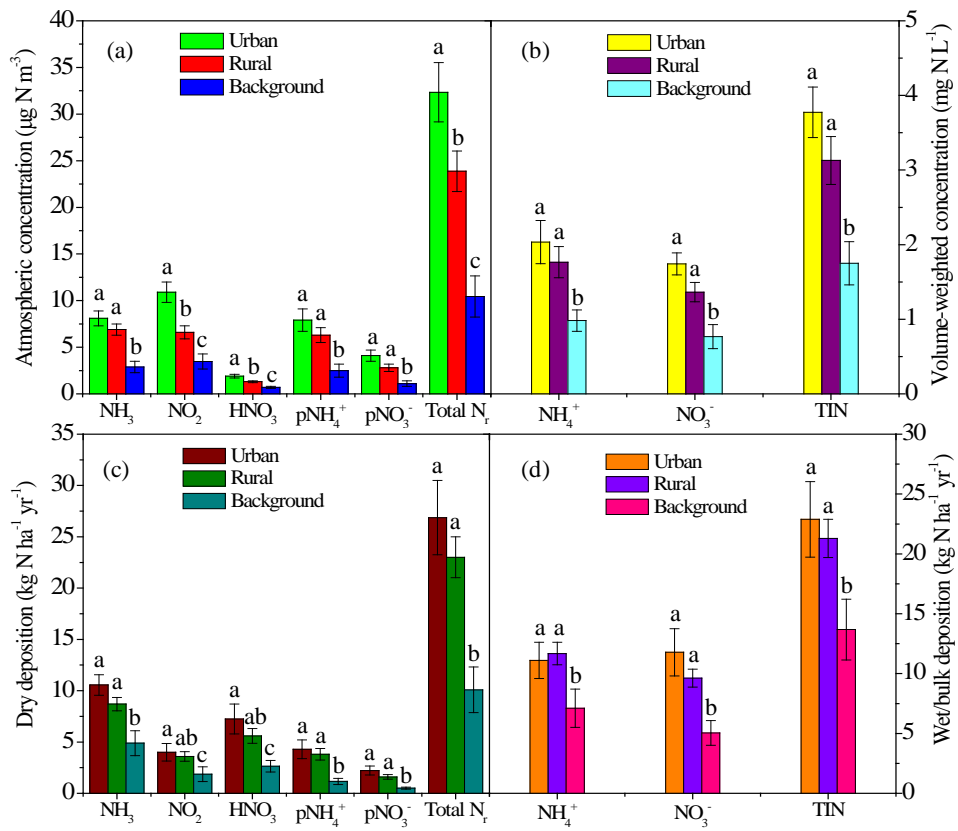
1155

1156

1157

1158

1159 **Figure 4**



1160

1161

1162

1163

1164

1165

1166

1167

1168

1169

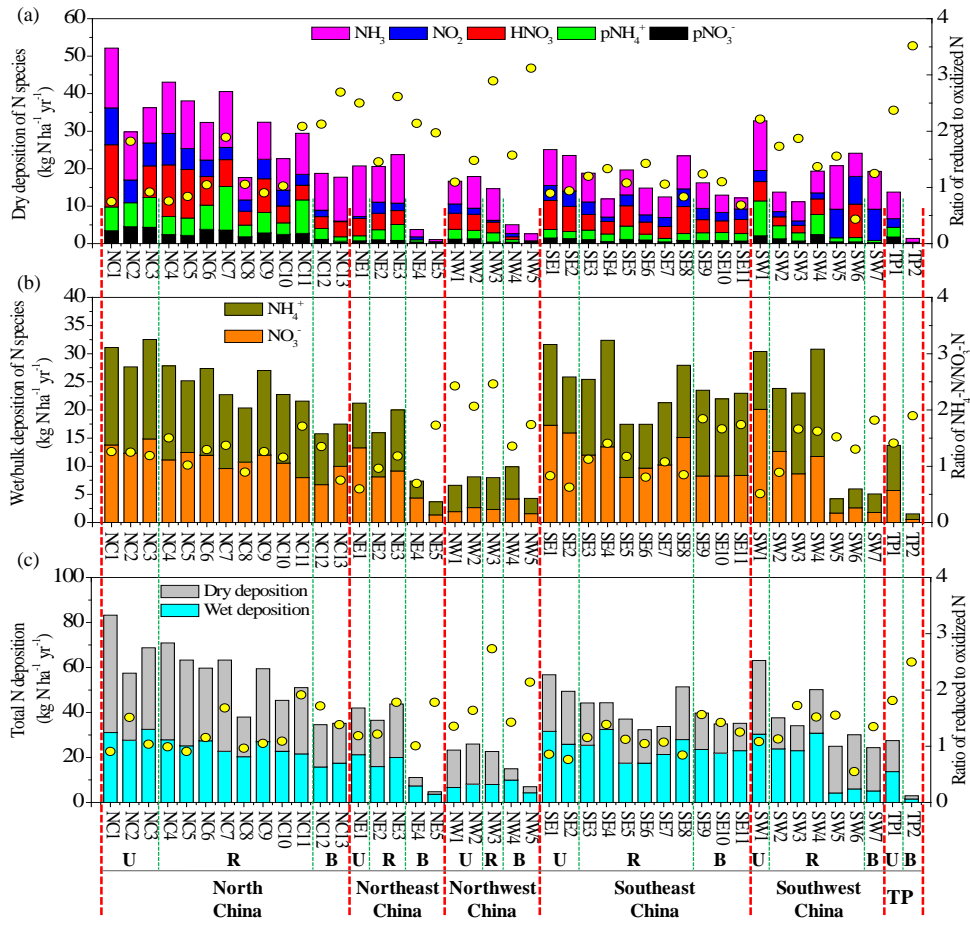
1170

1171

1172

1173

1174 **Figure 5**



1175

1176

1177

1178

1179

1180

1181

1182

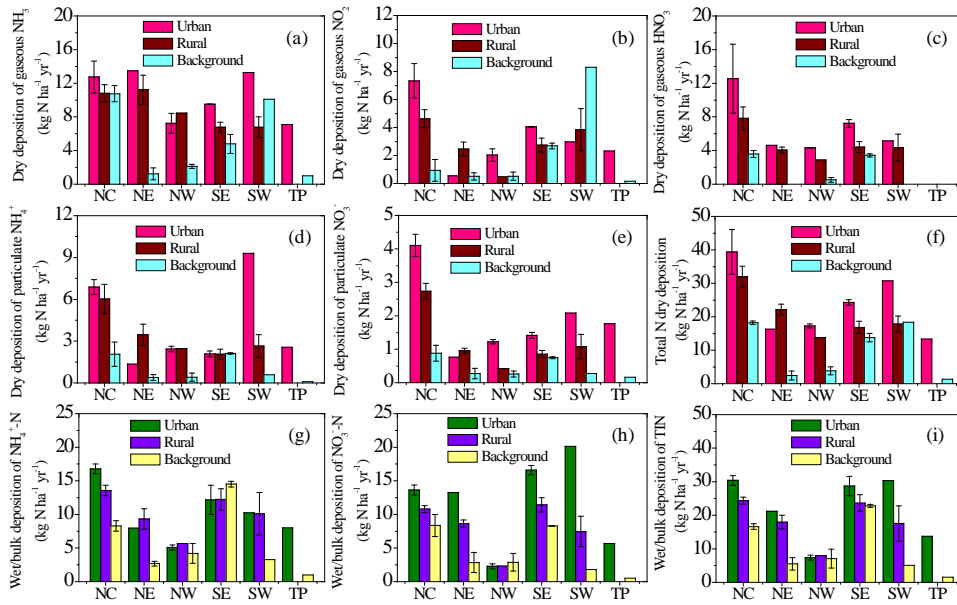
1183

1184

1185

1186

**Figure 6**



1188

1189

1190

1191

1192

1193

1194

1195

1196

1197

1198

1199

1200

1201

1202

1203

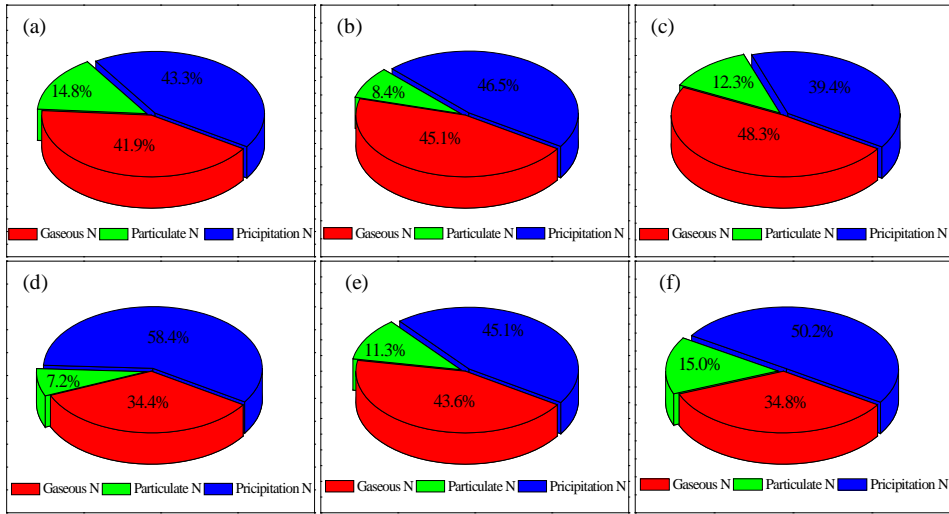
1204

1205



1206

Figure 7



1207

1208

1209

1210

1211

1212

1213

1214

1215

1216

1217

1218

1219

1220

1221

1222

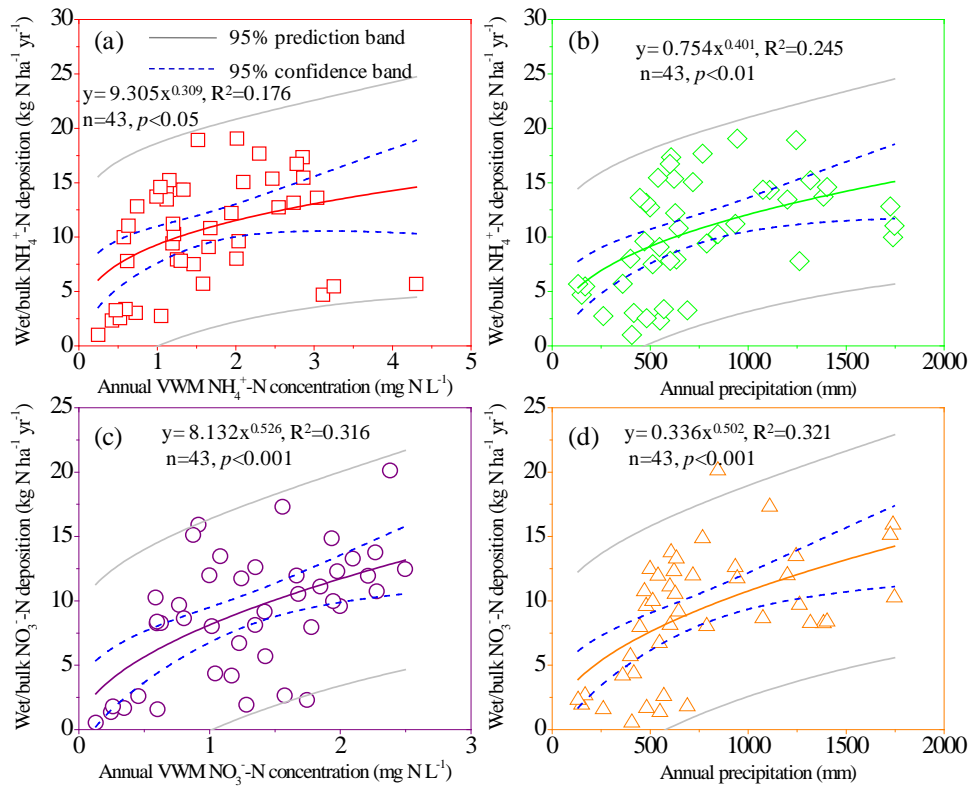
1223

1224

1225

1226

1227

**Figure 8**

1229

1230

1231

1232

1233

1234

1235

1236

1237

1238

1239

1240

1241

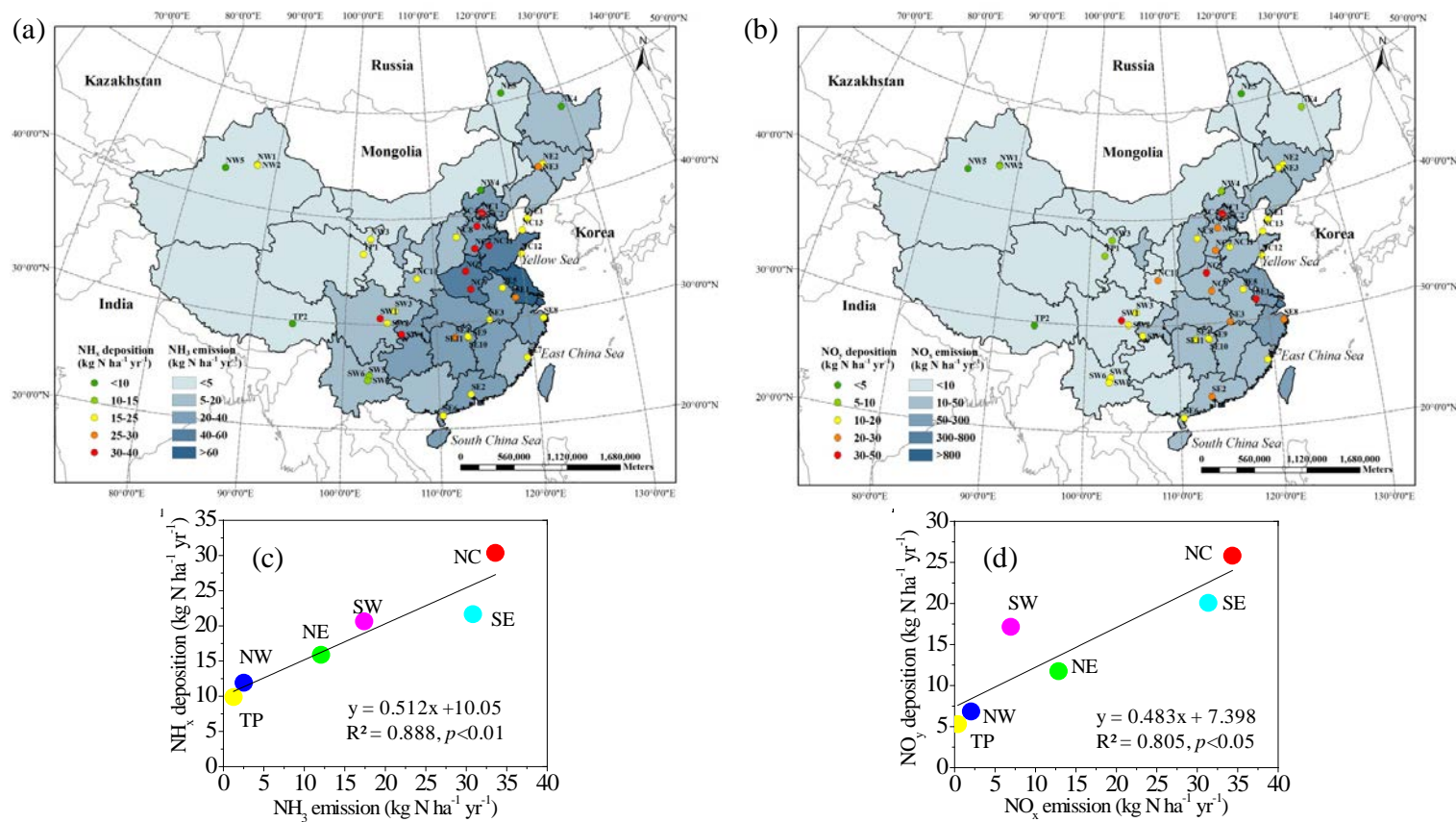
1242

1243

1244

1245

1246 **Figure 9**



1248 **Table 1.** Comparison of dry, wet (wet/bulk), and total deposition fluxes of N<sub>r</sub> compounds between NNDMN in China and 3 networks in other  
1249 countries.

Network	Japan EANET network <sup>a</sup>			CASTNET <sup>b</sup>			EMEP <sup>c</sup>			NADMM <sup>d</sup>			
Number of sites or grids	10 sites			130 sites			2447 grids (0.5° × 0.5°)			33 sites			
Observation period	Apr. 2003-Mar. 2008			Apr. 2006-Dec. 2013			Jan. 2003-Dec. 2007			Aug. 2006-Sep. 2014			
N deposition (kg N ha <sup>-1</sup> yr <sup>-1</sup> )	Dry	Wet	Total	Dry	Wet	Total	Dry	Wet	Total	Dry	Wet/bulk	Total	
	Average	3.9	6.6	10.6	3.1	1.3	4.4	3.9	4.8	8.7	18.7	18.2	36.9
	Median	4.1	5.9	11.2	3.0	0.7	4.1	3.7	4.7	8.5	18.7	21.3	36.5
	Max	7.0	15.8	18.2	9.7	10.3	19.6	15.8	16.9	28.0	43.1	32.4	70.9
	Min	1.0	2.1	3.0	0.03	0.1	0.3	0.1	0.6	0.7	1.1	1.5	2.9

1250

1251 <sup>a</sup>The Japan EANET data are sourced from [Endo et al. \(2011\)](#). Gaseous NO<sub>2</sub> was not included in estimates of dry N deposition.

1252 <sup>b</sup> The CASNET data are available online (<http://www.epa.gov/castnet/>). Gaseous NH<sub>3</sub> was not included in estimates of dry N deposition.

1253 <sup>c</sup>The EMEP data are sourced from [Endo et al. \(2011\)](#), in which the dry and wet deposition amounts at each grid covering 27 EMEP countries  
1254 were estimated by the unified EMEP models ([Simpson et al., 2003](#)).

1255 <sup>d</sup> Only including the rural and background sites in NNDMN.  
1256  
1257

域代码已更改

带格式的: 字体: (中文) + 中文正文, 无下划线

带格式的: 字体: (默认) + 西文正文, (中文) + 中文正文, 无下划线, 字体颜色: 自动设置